



INSTITUT DE FRANCE
Académie des sciences

Comptes Rendus

Chimie

Dominique Bazin

Nanomaterials in medicine: a concise review of nanomaterials intended to treat pathology, nanomaterials induced by pathology, and pathology provoked by nanomaterials

Volume 25, Special Issue S3 (2022), p. 165-188

Published online: 11 August 2022

<https://doi.org/10.5802/crchim.194>

Part of Special Issue: Active site engineering in nanostructured materials for energy, health and environment

Guest editors: Ioana Fechete (Université de Technologie de Troyes, France) and Doina Lutic (Al. I. Cuza University of Iasi, Romania)



This article is licensed under the
CREATIVE COMMONS ATTRIBUTION 4.0 INTERNATIONAL LICENSE.
<http://creativecommons.org/licenses/by/4.0/>



Les Comptes Rendus. Chimie sont membres du
Centre Mersenne pour l'édition scientifique ouverte
www.centre-mersenne.org
e-ISSN : 1878-1543



Active site engineering in nanostructured materials for energy, health and environment /
*Ingénierie de sites actifs dans les matériaux nanostructurés pour l'énergie, la santé et
l'environnement*

Nanomaterials in medicine: a concise review of nanomaterials intended to treat pathology, nanomaterials induced by pathology, and pathology provoked by nanomaterials

Dominique Bazin^{® a}

^a Institut de Chimie Physique, UMR CNRS 8000, Bâtiment 350, Université Paris Saclay,
91405, Orsay cedex, France
E-mail: Dominique.bazin@universite-Paris-Saclay.fr

Abstract. This contribution is a concise review of nanomaterials in medicine, those designed to treat pathology, those which are induced by pathology, and those which provoke pathology. Clearly, there is a vast family of therapeutic and medically relevant nanomaterials, to which numerous excellent journals and books are dedicated. The purpose of the first section is to illustrate the chemical complexity of research into therapeutic nanomaterials and the challenges in their characterisation. The second section treats that family of nanomaterials induced by diverse pathologies, such as metabolic disorders, infection, or cancer. Here, the challenge is to find characterisation techniques able to provide chemical information at the nanometer scale to enable and enhance early medical diagnosis. Finally, various nanomaterials injected into the human body for esthetic purposes are discussed, specifically tattoo inks which can provoke severe pathologies such as skin cancer.

Keywords. Pathological calcifications, Nanomaterials, Medicine, Characterization techniques, Nanomedicine, Nanotechnology, Theranostics.

Published online: 11 August 2022

1. Introduction

This manuscript forms part of a special issue dedicated to the research of Professor E. Dumiriu, focused on the relationship between nanomaterials and medicine [1–4]. According to the European Commission, “Nanomaterial” means: “A natural, incidental or manufactured material containing particles, in an unbound state or as an aggregate or as an agglomerate and where, for 50% or more of

the particles in the number size distribution, one or more external dimensions is in the size range 1 nm–100 nm. In specific cases and where warranted by concerns for the environment, health, safety or competitiveness the number size distribution threshold of 50% may be replaced by a threshold between 1 and 50%. By derogation from the above, fullerenes, graphene flakes and single wall carbon nanotubes with one or more external dimensions below 1 nm should be considered as nanoma-

terials" [5]. Here, three kinds of nanomaterials are considered.

First, we will consider the development of nanomaterials for the treatment of severe pathologies, to improve prognosis through a synergistic combination of diagnosis and therapy, thereby facilitating personalized medicine [6,7]. As underlined by a recent European community report [8], several medical specialties can benefit from such nanomaterials. Among them, we can cite oncology, immunology, dermatology, neurology, ophthalmology, and urology. Clearly, the number of nanomaterials used in nanomedicine is huge and numerous excellent journals and books are devoted to this subject [9,10]. Accordingly, only a concise review will be presented regarding the chemical diversity of such nanomaterials. Also, to illustrate the complexity of characterization in biological tissues, some data is presented on so-called "quantum rattles" (QRs) based on AuQDs (quantum dots) and gold nanoparticles (NPs) confined in mesoporous silica, which are claimed to improve prognosis via a single multifunctional agent [11,12].

The second family of nanomaterials of medical significance discussed has endogenous origins and is induced by certain pathologies. As previously emphasized [13,14], microcrystalline pathology is an exciting research field in which most investigations have been performed on the mineral component of pathological calcifications. Various pathologies including cancer [15,16], infection [17–19], and genetic disorders [20–25], may generate nanomaterials. In these cases, the challenge is not related to the development of new nanomaterials but to developing characterisation techniques able to provide chemical information at the nanometer scale for early medical diagnosis [26–28].

The third family of nanomaterials discussed is those purposefully injected into the human body and associated with the art of tattooing which has served extremely diverse purposes [29]. According to the historian Herodotus (484–426 BC), ancient Greeks learned both the idea of penal tattoos and the art of tattooing from the Persians around the sixth century BC [29]. Tattooing involves introducing pigmented material into the dermis by puncturing the skin to generate a permanent design. Nowadays, most tattoo inks synthetic substances [30,31] in which various types of nanomaterials have been identified. A

publication of Colboc *et al.* [32] of an investigation of the chemical composition and distribution of tattoo inks within tattoo associated keratoacanthoma (KA) is discussed. Note that tattooing of cosmetically disfiguring corneal scars may be a valuable therapeutic alternative to reconstructive surgical procedures in a distinct group of patients where the latter will not result in functional improvement or carry the risk of phthisis [33].

2. Nanomaterials dedicated to the treatment of pathologies

The definition of nanomedicine given by the European Science Foundation in 2004 is "the science and technology of diagnosing, treating, and preventing disease and traumatic injury, of relieving pain, and of preserving and improving human health, using molecular tools and molecular knowledge of the human body" [34].

2.1. The huge chemical diversity of nanomaterials

As underlined by Min *et al.* [35], research in nanomedicine has already led to the development of a wide range of products including therapeutics, diagnostic imaging agents, in vitro diagnostics, and medical devices. This versatility obviously arises from the wide chemical diversity among medical nanomaterials. Nanomedicine effectively began with liposomes as the first therapeutic NP platform [36]; Figure 1 illustrates several more to be considered [37,38].

To illustrate the huge chemical diversity of medical nanomaterials, consider those platforms based on metal particles. Various metals (Table 1) namely Aluminium, Cobalt, Copper, Gold, Iron, Silver, Titanium can be used in cancer immunotherapy contexts [39].

This is also true of antimicrobial activity; metal oxide nanomaterials such as zinc oxide (ZnO), iron oxide (Fe_3O_4), copper oxide (CuO), magnesium oxide (MgO), and titanium dioxide (TiO_2) NPs possess antimicrobial activity towards a range of Gram-positive

Table 1. Overview of the variety of NPs containing metals and examples of their cancer immunotherapy applications [39]

Aluminium oxide	Adjuvant	Enhances anti-cancer effects of tumor cell vaccines	Observed smaller tumor sizes and more CTL) when co-administered with a tumor cell vaccine
Cobalt oxide	Antigen delivery	Induces macrophage activation	Increased antigen-specific CTLs <i>in vivo</i>
Cuprous oxide	Alter tumor microenvironment	Alter expression of drosophila transcription factor	Induced myeloid infiltration and systemic immunity
Gold	Antigen/adjuvant delivery; Photothermal therapy	Increased CTL responses; tumor ablation released tumor antigens	Reduced tumor growth <i>in vivo</i> ; prevented tumor growth <i>in vivo</i>
Iron oxide	M1 macrophage polarization; Protein delivery; Photothermal therapy	Increased pro-inflammatory macrophage proliferation; IONP-HSP chaperoned antigens to APCs; thermal tumor ablation	Inhibited tumor growth; IONP-HSP70 led to tumor-specific CTL responses; ablation led to protective immunity
Silver	Reduce tumor-promoting cytokines	Decreased IL-1 β signaling in tumor microenvironment	Inhibited fibrosarcoma tumor growth <i>in vivo</i>
Titanium dioxide	Immune stimulation induced by ultrasound	ROS generation increased pro-inflammatory cytokines and interleukins in the tumor	Suppressed tumor growth <i>in vivo</i>
Zinc oxide	Antigen delivery (pulsed DCs)	Improved antigen-specific CTL responses	Delayed tumor growth <i>in vivo</i>

CTL: cytotoxic T lymphocyte. IONP: iron oxide nanoparticle. HSP: heat shock protein. IL-1 β : interleukin 1 beta. ROS: reactive oxygen species. DC: dendritic cell. APC: antigen presenting cell.

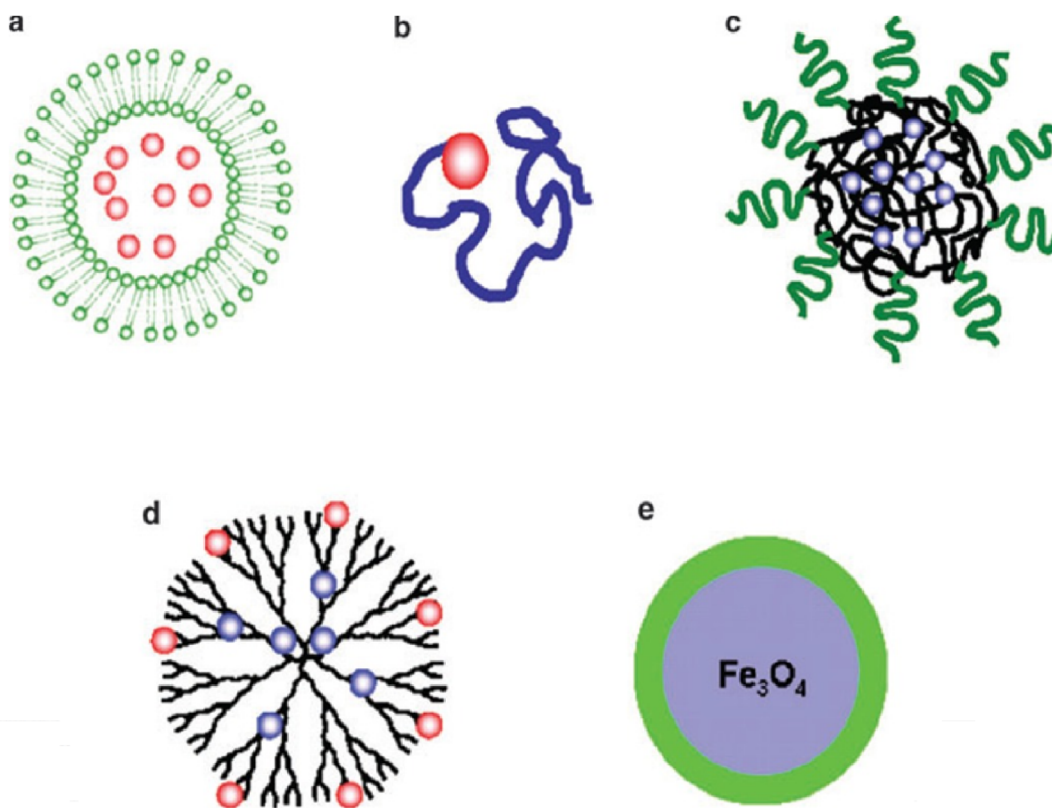


Figure 1. Schematic illustration of therapeutic NP platforms in preclinical development: (a) liposome, (b) polymer–drug conjugate, (c) polymeric NP, (d) dendrimer, and (e) metal oxide NP (here iron oxide). The red dots represent hydrophilic drugs and the blue dots represent hydrophobic drugs (from Zhang *et al.* [37]).

and Gram-negative bacteria, including resistant bacterial strains [40]. Note that their antibacterial activity is usually related to the generation of reactive oxygen species (ROS), attributed to their intrinsic photocatalytic activity or to the release of the metallic ions [41,42].

2.2. *The huge diversity of the physicochemical properties of a single kind of nanomaterial*

For one type of the NPs discussed here, gold NPs, morphological modification leads to modulation of properties (Figure 2) [43]. As shown in Figure 2, AuNPs can be used in tissue engineering for improving scaffold mechanical properties, electrical coupling between cells, and cell adhesion, and for promoting stem-cell proliferation, differentiation and maturation.

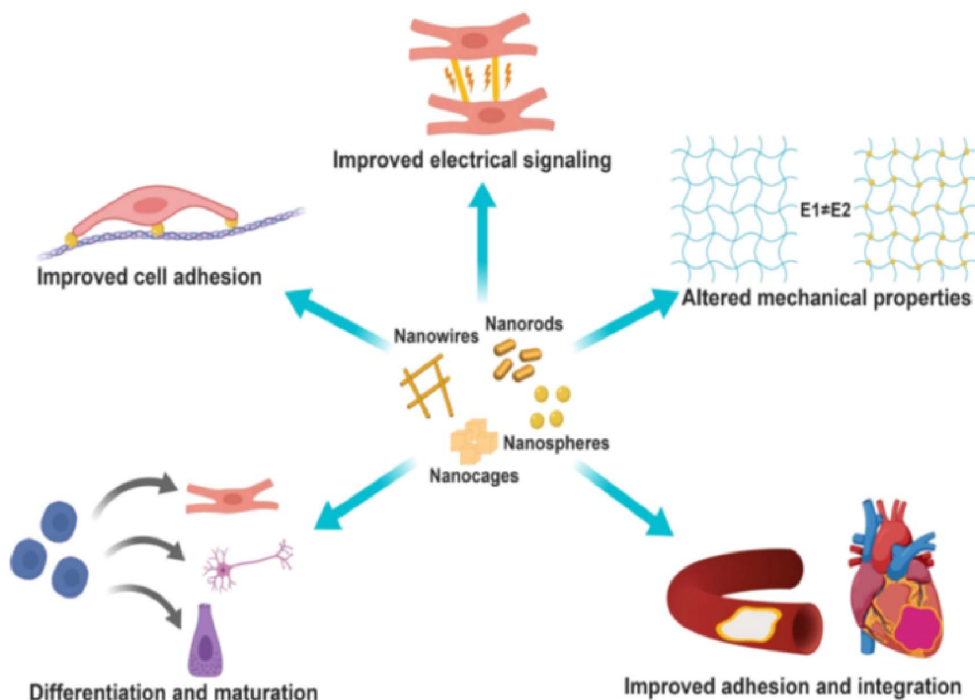


Figure 2. Uses of AuNPs in tissue engineering. AuNPs can be synthesized in various shapes and sizes, which dictate their physical properties and make them suitable for various applications [43].

AuNPs also offer the possibility for surface adsorption of molecules for a variety of purposes (Figure 3). These include antibodies, biopolymers such as collagen, or monolayers of small molecules to render the NPs biocompatible, as discussed by Salata [44] (Figure 3).

2.3. The extensive diversity of synthetic methodology

Finally, it is worth pointing out the different synthesis methods [45–48] developed to produce nanomaterials. These fall into two major categories: “bottom-up” and “top-down” approaches (Figure 4). The difference between them can be readily illustrated by nanoclusters (NC), a subset of materials which bridge the gap between NPs and atoms. In this case, the formation of NCs by assembly of ions or atoms, or the etching of NPs to smaller NCs, exemplify the “bottom-up” and the “top-down” approaches respectively [49].

To illustrate aspects of medical nanomaterials research, we discuss theranostic vectors consisting of gold clusters included in mesoporous silica spheres [11,12,50]. A precise characterization of the nanomaterials is the first requirement. Figure 5 shows negative mode electrospray-ionization mass spectrometry results of $[\text{Au}_{25}(\text{aminothiophenol or ATP})_{18}]^{-}$ clusters dissolved in dimethyl sulfoxide at $1 \text{ mg}\cdot\text{mL}^{-1}$. The negative-ion mass spectrum is dominated by two peaks (Figure 5), the first one near $m/z = 7160$ which corresponds to the $\text{Au}_{25}(4\text{ATP})_{18}$ cluster and the second one around $m/z = 3600$ which corresponds to a doubly charged Au_{25} cluster with some ligands further reacted (corrupted). This is consistent with the average particle diameter ($1.2 \pm 0.3 \text{ nm}$) deduced from transmission electron microscopy (TEM) (Figure 5), in which small black points, corresponding to Au clusters, are visible inside large silica spheres of 100 nm .

To fabricate these theranostic vectors, gold clusters were added to the mesoporous silica sphere solution and stirred overnight in water at room temperature. The resulting solid “quantum rattles” (QRs) based on gold quantum dots (AuQDs) was washed

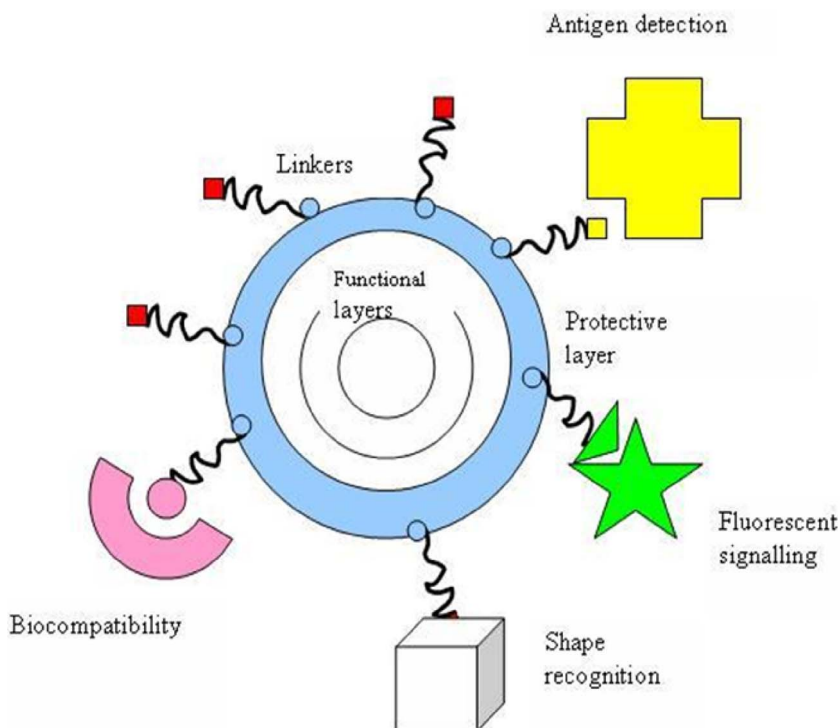


Figure 3. Typical configurations utilised in biomedical nanomaterials [44].

with water three times using sequential centrifugation and ultrasonic dispersion. Intravenous injection was performed under isoflurane anesthesia (3.5% induction, 1.5% retention) to reduce stress and pain.

After injecting the theranostic vectors/nanoparticles, it is very important to define their distribution across different organs. To this end, when the nanomaterials contain heavy elements, XRF is a unique tool [51,52]. It relies on the emission of characteristic secondary X-rays by specific atoms after irradiation by high energy X-rays [53]. The key point is that the energy of the emitted photon is specific to the photo-excited atom [54].

A typical X-ray fluorescence of a biological tissue containing QRAuQDs is shown in Figure 6. They give rise to the Au L_{α} emission; the experimental conditions, in air, do not show the expected silica X-ray fluorescence [55,56]. The high spatial resolution (between 10 μm and 30 μm) of synchrotron XRF [56], enables rapid (around 30 ms) maps of the different elements to be constructed [11].

Figure 7 plots the spatial distribution of different elements in kidney. It is important to differentiate elements present in the kidney from those in the embedding paraffin, which a quick visual inspection indicates as Cr, Ti, V and Ni.

Finally, it is worth to point out a possible spatial correlation between Zn and Au. Zinc, established as an essential trace element in 1961 [57] participates in regulating the physiological anti-inflammatory response [58]. To assess a possible inflammation process induced by QRAuQDs theranostic vectors, data on the spatial repartition of QR-AuQDs particles (based on the intensity of the X-ray fluorescence Au L_{α}) have been acquired and compared to Zn spatial distribution (Zn K_{α} emission) for the rat kidney (Figures 8a and 8b), spleen (Figures 8c and 8d) and liver (Figures 8e and 8f).

Although visual inspection suggests a spatial correlation between Zn and Au, the Pearson and Manders correlation coefficients [59,60] are both 0.7, and not close to 1 (Figure 9). This means that Zn-Au distributions are not strongly linked and there is no strong correlation between Au distribution and in-

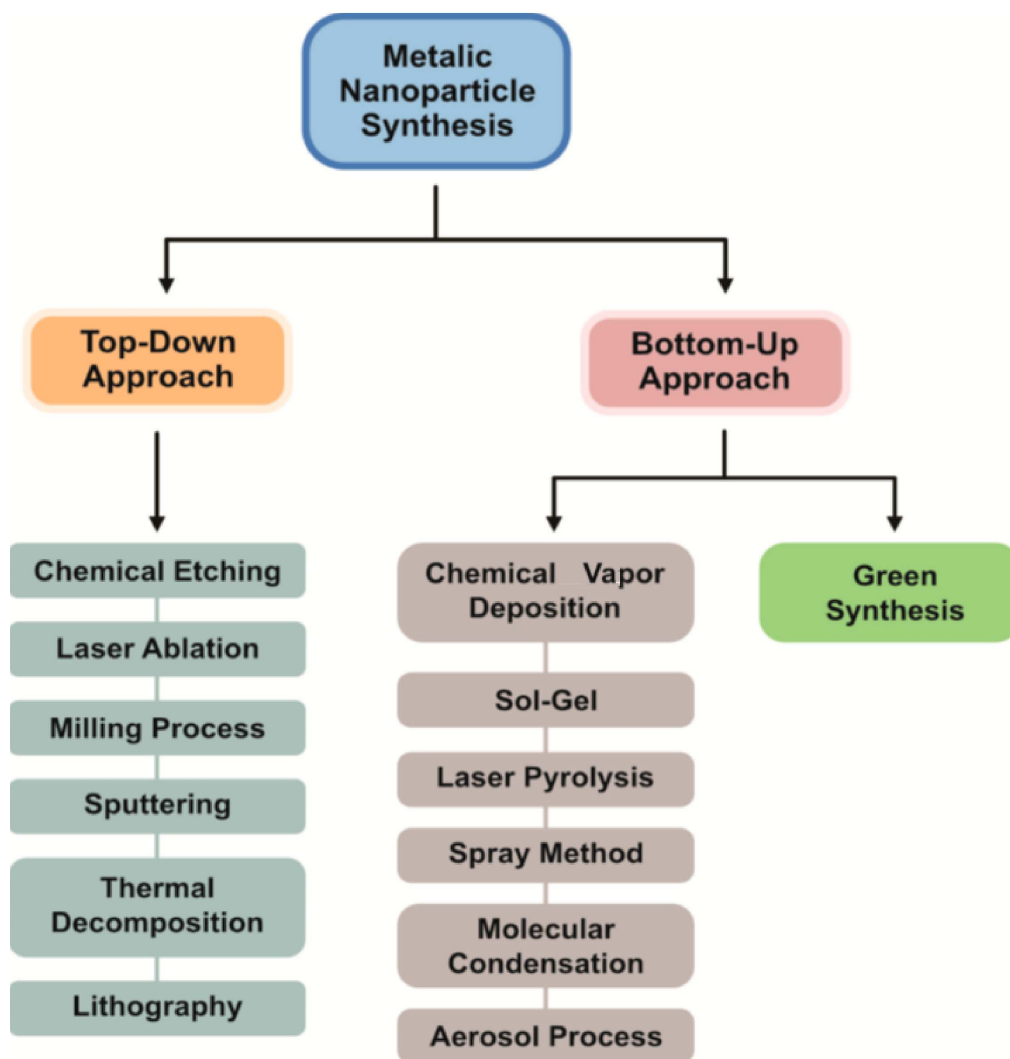


Figure 4. Conventional methods for NP synthesis [45–48].

flammation, unlike the case for cisplatin [61,62], an anti-cancer drug associated with significant nephrotoxicity. This is consistent with the literature showing that silica generated through “soft” chemistry does not provoke an inflammatory response.

This example shows clearly that the synthesis of bionanomaterials as well as their characterization in biological tissues constitute a significant challenge.

3. Pathology-induced nanomaterials

Several diseases including cancer, genetic disorders, cardiovascular abnormalities, or infection, can provoke pathogenic calcifications in various tissues [63–67]. Pathological calcifications exhibit several levels of organization [13,14] resulting from agglomeration of crystallites (of typically micrometer dimensions and observable by Scanning Electron Microscopy (SEM)), in which each crystallite appears to be composed of nanocrystals (of dimensions typi-

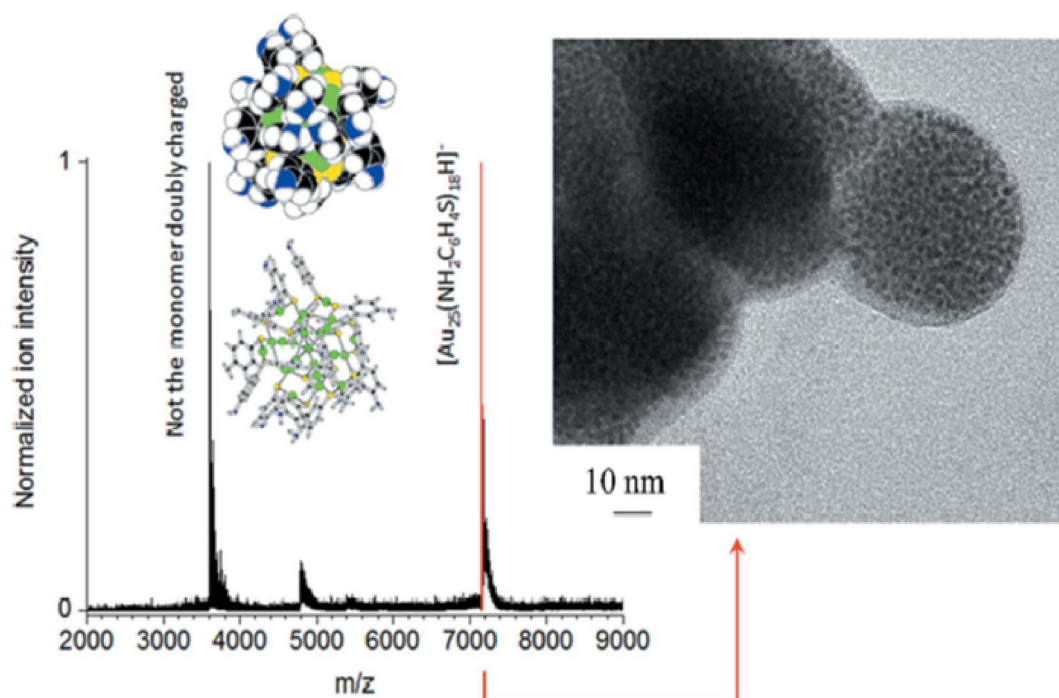


Figure 5. Electrospray-ionization mass spectrometry (SYNAPT G2S-HDMS mass spectrometer equipped with an electrospray ionization source) and TEM image (FEI Tecnai G2 Spirit instrument operating at an acceleration voltage of 120 kV) of the $\text{Au}_{25}(\text{4ATP})_{18}$ clusters. Clusters were dispersed in dimethyl sulfoxide for analysis (from Esteve *et al.* [11]).

Table 2. Selected chemical compounds most frequently identified in kidney stones (\square is for vacancy)

Chemical compounds with calcium	
Whewellite	$\text{CaC}_2\text{O}_4 \cdot \text{H}_2\text{O}$
Weddelite	$\text{CaC}_2\text{O}_4 \cdot 2\text{H}_2\text{O}$
Brushite	$\text{CaHPO}_4 \cdot 2\text{H}_2\text{O}$
Apatite	$\text{Ca}_{10-x}\square_x(\text{PO}_4)_{6-x}(\text{CO}_3)_x(\text{OH})_{2-x}\square_x$ with $0 < x < 2$
Octacalcium phosphate	$\text{Ca}_8\text{H}_2(\text{PO}_4)_6 \cdot 5\text{H}_2\text{O}$
Chemical compounds without calcium	
Uric acid,	$\text{C}_5\text{H}_4\text{N}_4\text{O}_3$
7,9-dihydro-1H-purine-2,6,8(3H)-trione	
L-Cystine, 2-amino-3-(2-amino-2-carboxy-ethyl)disulfanyl-propanoic acid	$\text{L-C}_6\text{H}_{12}\text{N}_2\text{O}_4\text{S}_2$
Struvite, Magnesium ammonium phosphate	$\text{MgNH}_4\text{PO}_4 \cdot 6\text{H}_2\text{O}$
2,8-Dihydroxyadenine,	$\text{C}_5\text{H}_5\text{N}_5\text{O}_2$
6-Amino-1H-purine-2,8(7H,9H)-dione	

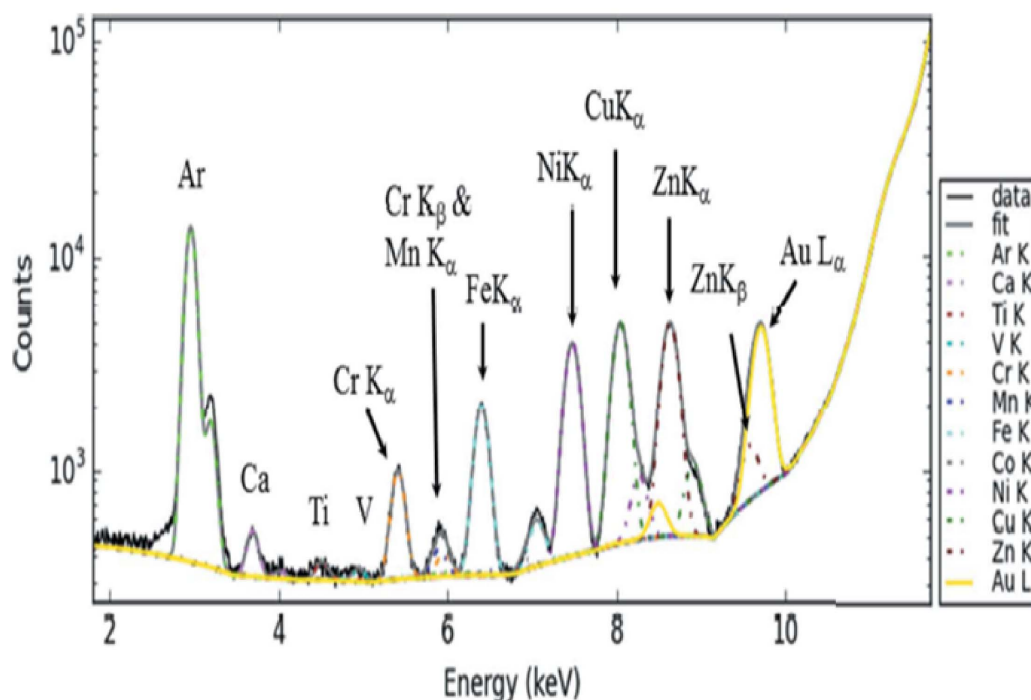


Figure 6. Typical X-ray fluorescence spectrum of a biological sample showing contributions from Ca (K_{α} at 3.691 keV, K_{β} at 4.012 keV), Fe (K_{α} at 6.404 keV, K_{β} at 7.058 keV), Zn (K_{α} at 8.638 keV, K_{β} at 9.572 keV) and Au (L_{α} = 9.713 keV) (from Esteve *et al.* [11]).

cally of some hundreds of nanometers which can be determined by X-ray or neutron diffraction). Scattering experiments clearly show that pathological calcifications can be considered as nanomaterials [68].

In the case of kidney, the morphoconstitutional model elaborated by Daudon [69–72] establishes a significant relationship between the physico-chemical characteristics of urinary stones and their pathogenic origin. This model takes into account the chemical composition and the crystalline architecture of urinary stones, which are usually very heterogeneous. Table 2 summarizes the chemical compositions of the phases most frequently identified in kidney stones (more than one hundred distinct chemical phases have actually been identified).

Over recent decades, there has been considerable interest in the application of such morphoconstitutional models to pathological calcifications in other

organs, namely prostate [73,74], thyroid [75–77], skin [78], breast [16,79] or joints [80–87].

3.1. Apatite nanomaterials identified in kidney

Based on extensive forensic studies between 1935 and 1938, Alexander Randall noticed, at the tip of the renal papillae, lesions consisting of calcium phosphate and carbonate deposits accumulating in the kidney interstitium [89]. Despite these seminal studies, this “Randall’s plaque” (RP) generated limited interest during the second part of the 20th century.

Current epidemiologic studies suggest that over recent decades RP-related stone prevalence has increased. In France, the proportion of stones harbouring an umbilication and typical plaques has increased threefold in recent years compared to three decades ago, especially in young patients [90]. More

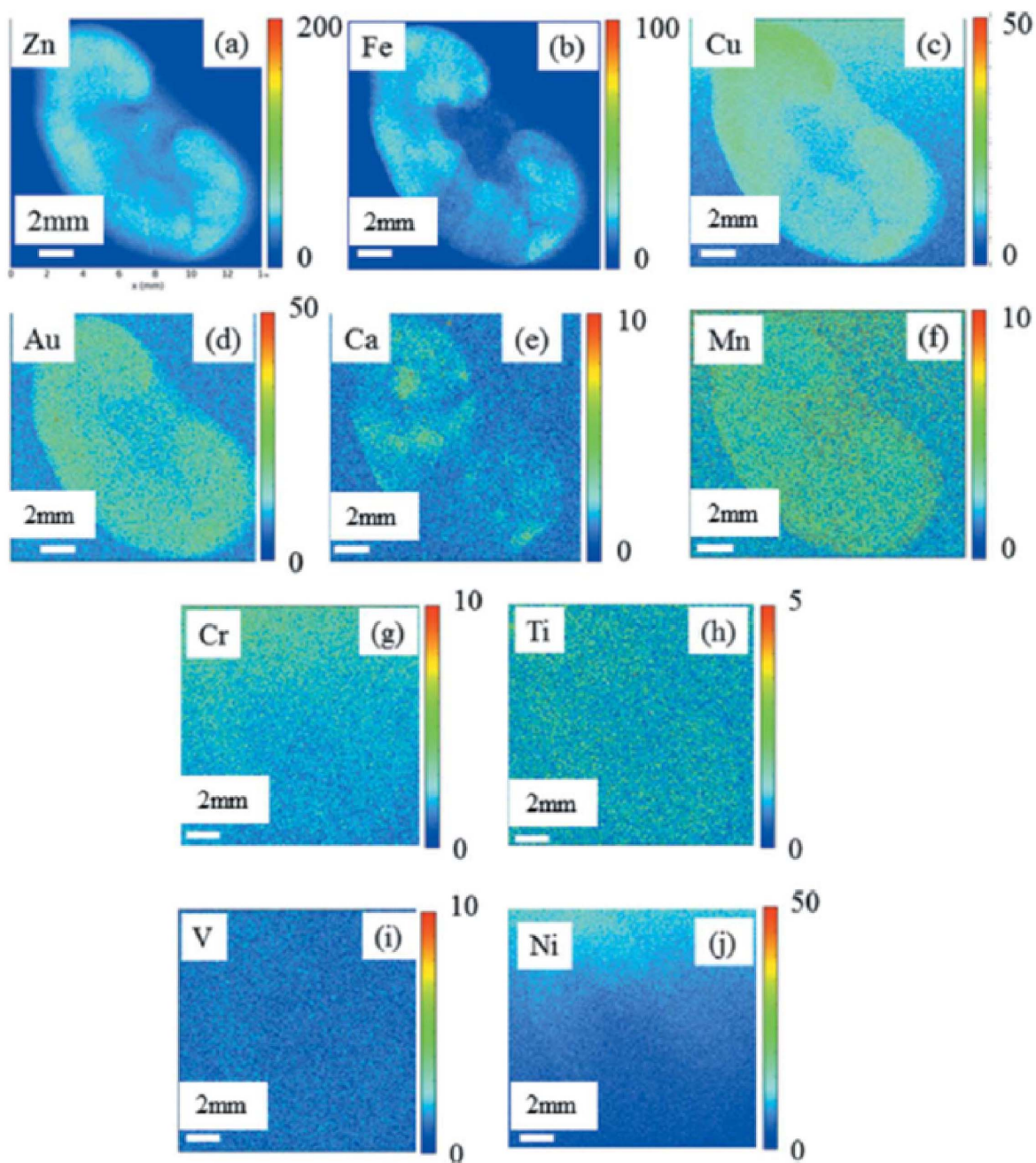


Figure 7. Spatial distribution of Zn (a), Fe (b), Cu (c), Au (d), Ca (e), Mn (f), Cr (g), Ti (h), V (i) and Ni (j), derived from their corresponding X-ray fluorescence emission lines (QR-AuQDs—exposed rat kidney embedded in paraffin); 13.7 mm \times 19.3 mm, 30 μ m resolution, 20 ms acquisition time) (from Esteve *et al.* [11]).

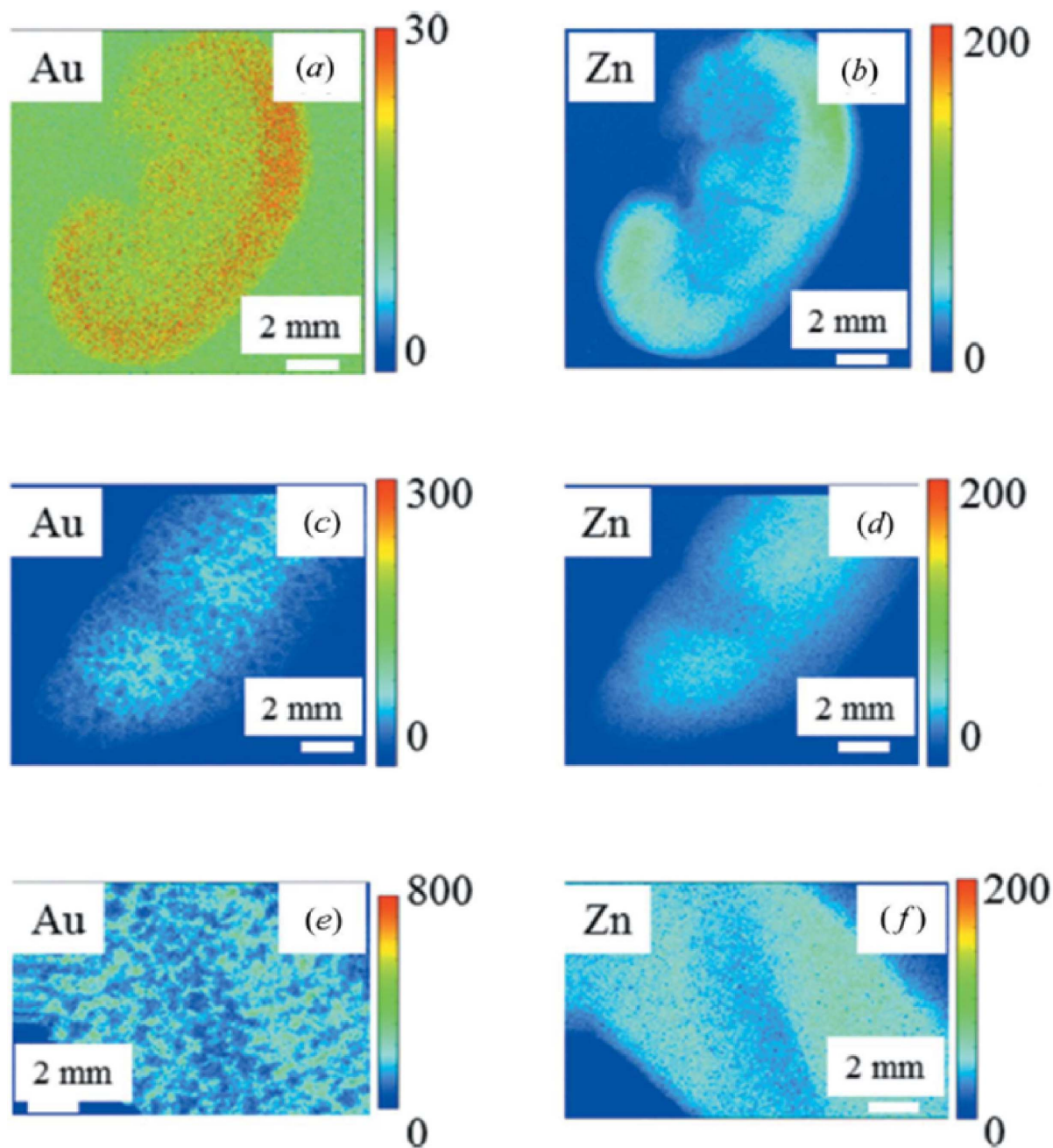


Figure 8. Spatial distribution of QR-AuQDs particles, and Zn, based on the intensity of the X-ray fluorescence Au L_{α} and Zn K_{α} emission for various rat organs: kidney (panels (a) and (b)), spleen (panels (c) and (d)) and liver (panels (e) and (f)) (from Esteve *et al.* [11]).

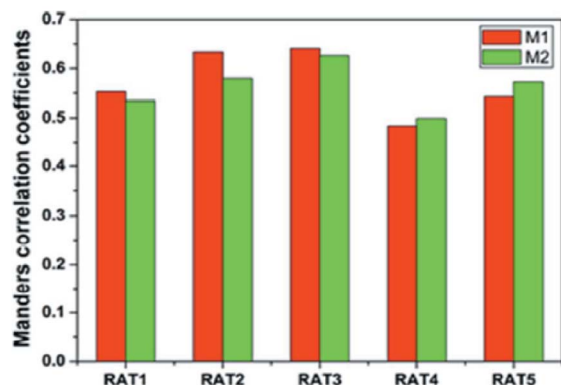


Figure 9. Manders coefficients for Au and Zn for the kidneys of all the animals used in this study (from Esteve *et al.* [9]).

specifically, children may develop calcium oxalate stones from calcium phosphatic apatite RP [91].

There are numerous excellent texts devoted to biological and synthetic calcium phosphate apatites [92–94]. With RP being of concern to the nephrologist and urologist, the RP literature is of great significance [88,95–105]. Figure 10 shows several X-ray diffraction patterns from RP samples; they are clearly similar to that from a calcium phosphate apatite kidney stone reference sample (sample N17105) [88].

The RP samples are primarily nanocrystalline apatites which display plate-like morphology (about 50 nm long, 25 nm width and 10 nm thick) and exhibit the usual anisotropy along the *c* axis [106]. These typical structural characteristics are associated in the X-ray diffractogram with a relatively fine (002) diffraction peak (at $2\theta = 26^\circ$) and several poorly resolved lines constituting a broad peak between $2\theta = 30^\circ$ and $2\theta = 35^\circ$. These structural characteristics are shared by numerous biological apatites associated not only with pathological but also with normal (bone, dentine) biocalcifications [106–108].

The physico-chemical characteristics of RP have implications in clinical practice. The close relationship between high urine calcium, and Randall's plaques, means that detecting a carbapatite plaque in an umbilicated calcium oxalate calculus points towards underlying hypercalciuria and/or low fluid intake.

Finally, it is worth to underline that calcium phosphate apatite pathological calcification appear as micrometer scale spherical entities. Previous investigations have show that the internal structure of spheri-

cal entities may display different configurations (Figure 11 from Ref. [109]). It can be supposed that concentric structures indicate that the pathogenesis of the calcification is made in a liquid environment.

3.2. Uric acid nanomaterials identified in kidney

Recent reports indicate that metabolic disorders associated with metabolic syndrome or type 2 diabetes predispose towards uric acid (UA) stones [110]. This is confirmed by Daudon *et al.* [111,112] who find that the proportion of UA stones is strikingly higher in stone formers with diabetes than those without.

To determine whether diabetic and non-diabetic patients form similar urinary stones, powder neutron diffraction (PND) experiments have been performed [113,114]. The fact that the neutron interacts only weakly with the stones and thus can penetrate deeply into the bulk offers an excellent opportunity for measuring the average size of the nanometre scale nanocrystals composed of light elements, as shown for other species identified in kidney stones [113].

A striking feature of the PND results (Figure 12) was that the crystal size of uric acid stones was significantly lower in diabetic patients (77.5 ± 5.3 nm vs. 105.8 ± 5.4 nm, $p = 0.0006$). This may be related to differences in urinary pH between diabetic and non-diabetic patients, as pH is the main factor explaining high UA supersaturation; in clinical practice, acidic urine was the main factor explaining UA stone formation [115].

3.3. Cystine nanomaterials identified in kidney

Cystinuria arises from a mutation in renal epithelial cell transporters, which induces a significant reduction in dibasic amino acids and cystine reabsorption and a high excretion of these amino acids, mainly lysine and cysteine [117–119]. Although cystinuria accounts for only 1%–2% of all urolithiasis and 6%–8% of urolithiasis in pediatric populations, repeated stone formation in affected patients often causes considerable morbidity [120].

The physicochemistry of twenty five cystine kidney stones were investigated by PND and scanning electron microscopy (SEM) [116]; Figure 13 shows a typical PND diffractogram.

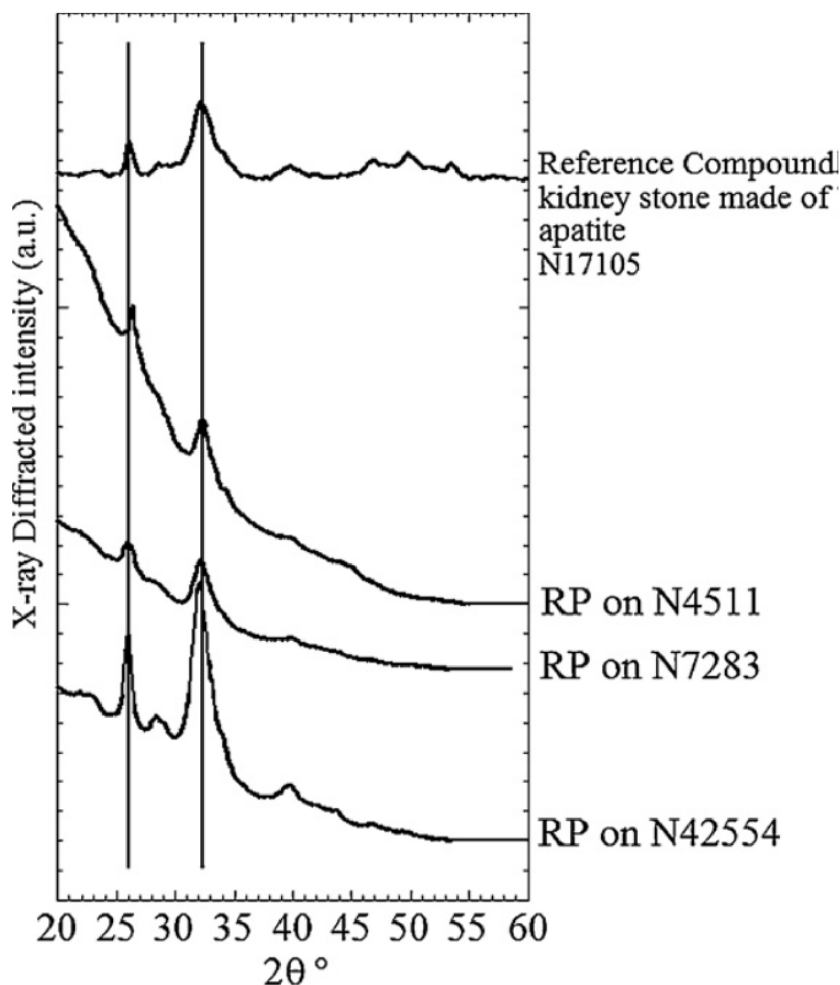


Figure 10. X-ray diffractograms from several RP samples, and a bio-apatitic KS reference standard (from Carpentier *et al.* [88]).

The mean crystal size was calculated for each sample using the FullProf software [116]. Patients treated by sodium bicarbonate alkalinization showed nanocrystals of significantly lower mean size. Patients on other treatments showed cystine surface modifications only. The structural characteristics of such cystine nanomaterials thus help the clinician assess therapy.

3.4. Calcium carbonate nanomaterials in skin

Sarcoidosis (Besnier-Boeck-Schaumann disease) is a multisystem inflammatory disease affecting different organs particularly lung, skin, eyes and joints [121,122]. Sarcoidosis, as well as being observed in

other granulomatous diseases, is associated with disorders of calcium metabolism [123]. Saidenberg-Kermanac'h *et al.* [124] have noticed that sarcoidosis patients have a high risk of fracture despite not having a lowered bone mineral density, suggesting that other independent factors are involved. As emphasised by Arkema and Cozier [125], sarcoidosis occurrence varies greatly by age and sex. What causes this variation is unknown, but it indicates that sex plays a role in the manifestation of disease. In some populations, there is a 10-year difference in age at diagnosis between men and women; in Sweden, the age at diagnosis in men was 45 compared with 54 in women [126].

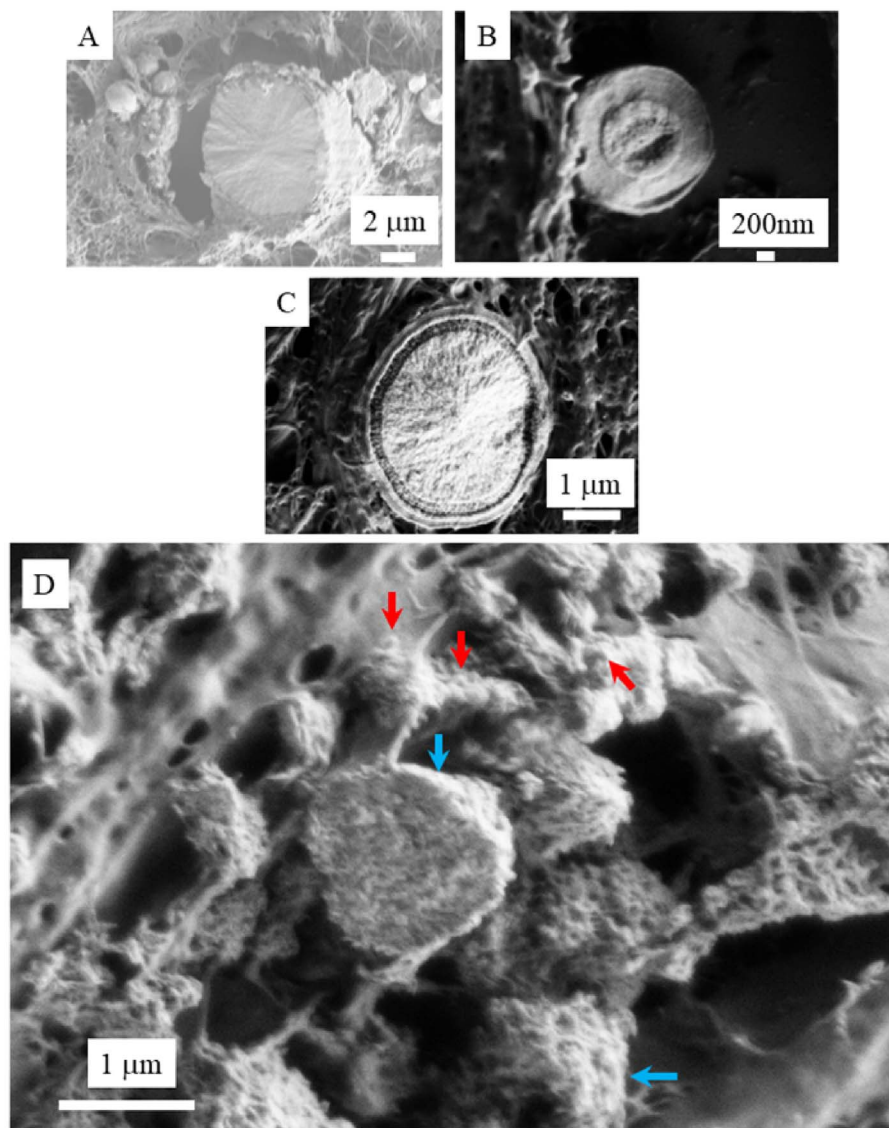


Figure 11. Spherical entities may display different internal structures: (A) Radial structures; (B) Concentric layers; (C) Both radial and concentric structure (A) to (C) images are breast calcifications). In the case of calcinosi cutis (D), micro-spherical entities (blue arrows) result of an agglomeration of nano-spherules (red arrows).

Colboc *et al.* [127] have investigated skin biopsies gather sarcoidosis related physicochemical data; SEM combined with Energy Dispersive X-ray Spectroscopy (Figure 14) and μ Fourier Transform InfraRed (FTIR) data [127] have given valuable information on calcium metabolism disorders.

Calcium metabolic disorders manifest nanometer scale spherical entities (Figure 14) made of calcite (a

form of calcium carbonate) at the periphery of the granulomas [127].

4. Nanomaterial-induced pathologies

Long perceived as a form of exotic self-expression in some social fringe groups, tattoos have shed their

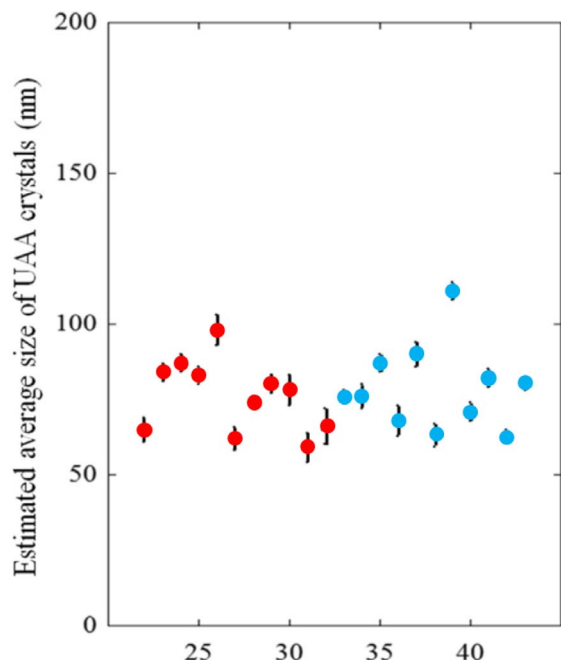


Figure 12. Nanocrystal sizes of UAA urinary stones from diabetic male (from 22 to 32 in red circles) and female (from 33 to 43, blue circles) patients (from Daudon *et al.* [112]).

maverick image and become mainstream, particularly for young people [130]. It is important to note that in permanent tattoos and permanent make-up, the pigments are deposited into the dermis by means of a needle (Figure 15) [128,129].

This process ensures that the pigments cannot be removed. Simultaneously the organism is exposed to the pigments in the tattoo in a very direct way and for a prolonged time [131]. Health problems have arisen from the significant increase of available colours and thus pigments. In fact, the exact composition of tattoo inks is unregulated and often unknown [132].

Regarding the inorganic components of tattoo inks, Battistini *et al.* [133] have used SemiQuant Inductively Coupled Plasma Mass Spectrometry to characterise twenty inks of different brands and colours, and thus quantify 18 metals (Al, As, Ba, Cd, Co, Cr, Cu, Fe, Hg, Mn, Mo, Ni, Pb, Sb, Se, Sn, Ti, Zn). This technique also yielded the dimensions of the nanoscale metallic particles [133]. More specifically, Al was found at nano- (62–80 nm) and submicron-sizes (105–140 nm), Cr, Cu, Pb and Zn were in the

ranges 42–62 nm, 44–96 nm, 26–28 nm and 26–59 nm, respectively, and Ti in submicron range (166–383 nm).

Several publications using other techniques have confirmed this nanometer particle size. For example, Arl *et al.* [134] showed using dynamic light scattering that blue, green and red inks exhibited particle diameters above 200 nm and that black ink particles were smallest. Also, Høgsberg *et al.* [135] measured particle size by laser diffraction, electron microscopy and X-ray diffraction. Pigment sizes fell into three main classes. Black pigments were smallest and almost exclusively pure NPs (i.e. particles with at least one dimension <100 nm), white pigments the largest (TiO₂ pigment in the white inks had the smallest primary particle size of approximately 100 nm) and the coloured pigments intermediate between the two.

Various investigations have addressed nanomaterial accumulation in organs. Tang *et al.* [136] focused on two kinds of silver materials with different particle diameters (50–100 nm and 2000–20,000 nm) administered to rats via subcutaneous injection, showing clearly that the smaller reached the blood circulation and were distributed to the main organs, especially to the kidney, liver, spleen, brain and lung. In contrast, the larger ones were unable to invade the blood stream or organ tissue.

As pointed out by Battistini *et al.* [133], all these elements are present in the form of various oxides (Al₂O₃, Co₃O₄, Cr₂O₃, CuO, NiO, TiO₂, ZnO). Chemistry of tattoo inks can be accessed by vibrational spectroscopies such as FTIR [137,138] and Raman [139,140]. Yakes *et al.* [141] point out that, while pigment identification can be performed by using FTIR spectroscopy, Raman has the additional ability to identify carbon and some inorganic compounds that are challenging to detect with FTIR [142]. Raman spectroscopy also offers the ability to distinguish between the TiO₂ polymorphs anatase and rutile. Indeed, Colboc *et al.* [32] use Raman spectroscopy to demonstrate the presence of the TiO₂ rutile polymorph in a patient who presented a KA associated with a lighter shade of red, importantly because anatase and rutile differ in toxicity [143]. The same authors [32] have performed X-ray absorption Spectroscopy (XAS) experiments [144–147] to show the presence of zincite (ZnO) and goethite (α-FeOOH), as have Schreiber *et al.* [128,129] using synchrotron techniques. Thanks to the micrometer scale spatial

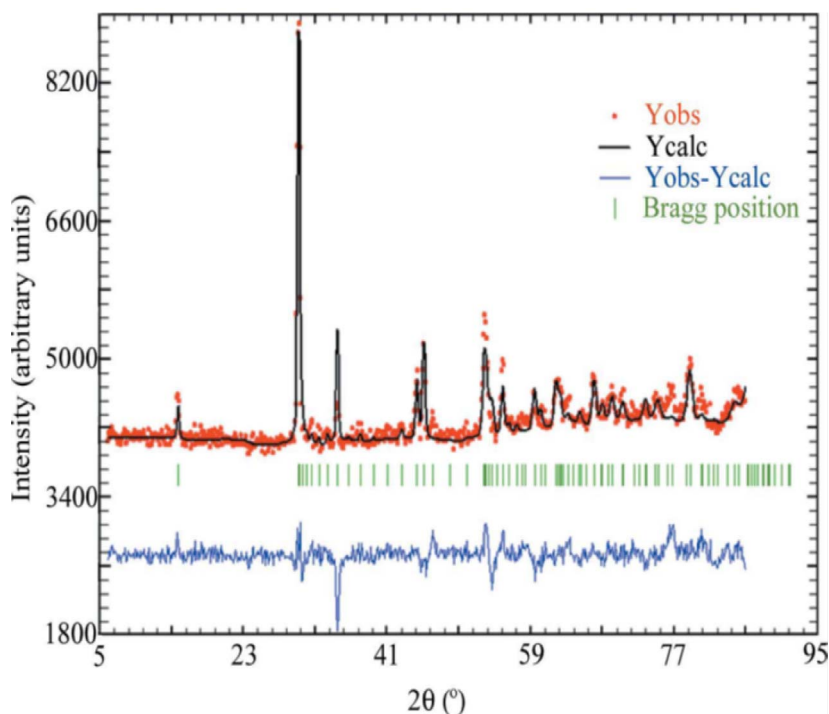


Figure 13. Typical observed (Yobs in red), calculated (Ycalc) and difference profiles (Yobs-Ycalc in blue) of the PND diagram of a cystine kidney stone. Tick marks (Bragg position in green) below the profiles indicate the peak positions of allowed Bragg reflections for cystine (from Bazin *et al.* [116]).

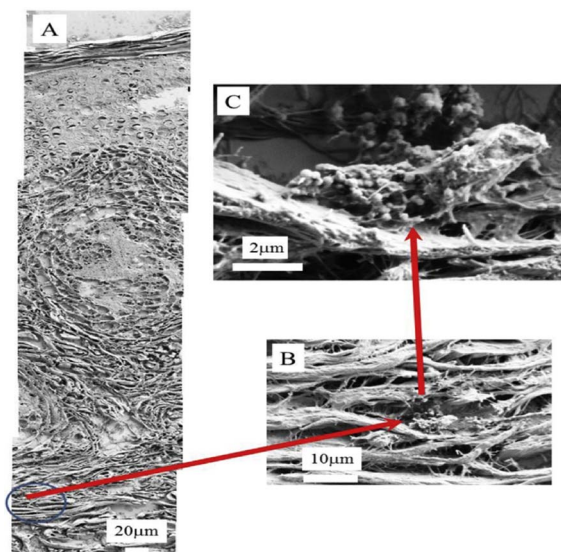


Figure 14. (A)–(C) SEM photographs at different magnifications. In (A), the three skin layers, the epidermis (50–100 µm), dermis (1–2 mm) and hypodermis (1–2 mm) can be seen.

resolution of XAS experiments [56,63,66,147,148], it is possible to correlate the optical image of tumors in skin biopsies with the spatial distribution of elements given by XRF data (Figure 16), helping the clinician to establish a significant relationship between pathology and the heavy elements in inks. Bear in mind at this point that the organic components of the ink must also be characterized.

For example, Colboc *et al.* [32] have measured a signal from the azo pigment (PR170) and from a TiO₂ particle in the very same area of a skin biopsy (Figure 17). It is possible that these two compounds in such close proximity induces some severe pathology. Generation of primary aromatic amines from azo pigments such as PR170 in humans is suspected to be the consequence of enzymatic activity, thermal decomposition, or photodegradation after exposure to UV light [149].

Finally, some cases of iatrogenic diseases may be due to the patient absorbing or generating nanomaterials. The literature contains several investigations

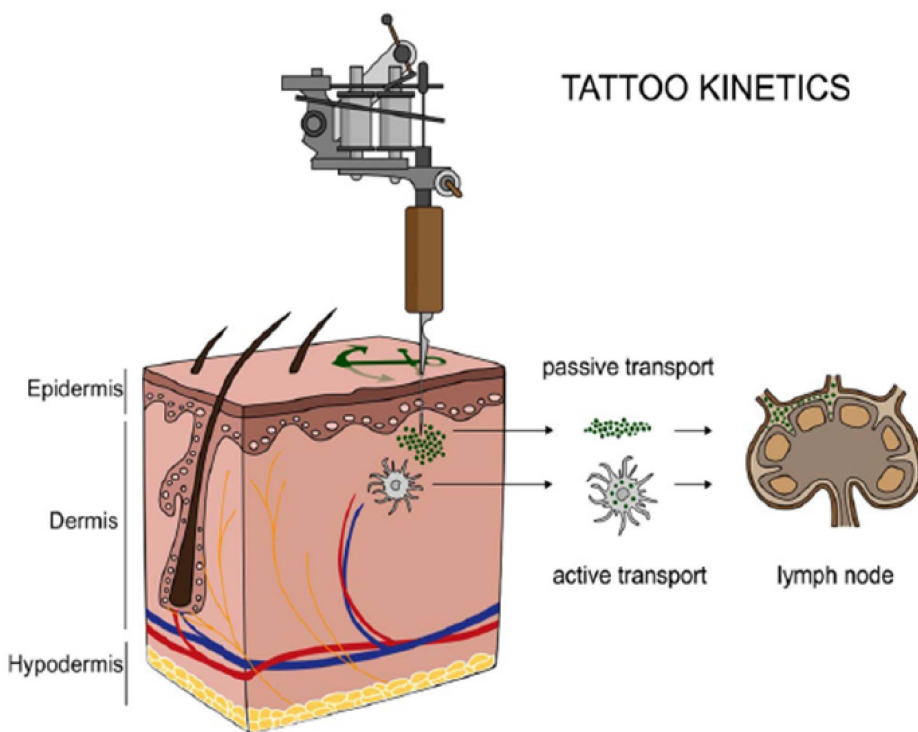


Figure 15. Translocation of tattoo particles from skin to lymph nodes. Upon injection of tattoo inks, NPs can be either passively transported via blood and lymph fluids or phagocytized by immune cells and subsequently deposited in regional lymph nodes. After healing, particles are present in the dermis and in the sinusoids of the draining lymph nodes. The picture was drawn by the authors (i.e., C.S.) (from Schreiver *et al.* [128,129]).

where abnormal deposits of drugs and their metabolites have been characterized [149–156].

5. Perspectives

For all the nanomaterials presented in this contribution, the emergence of in-lab characterization techniques yielding nanometer scale structural and chemical information represents a significant opportunity to increase understanding of their interaction with biological tissues [157].

Two possibilities exist to perform IR spectroscopy [137] beyond the diffraction limit i.e., to bridge the resolving power gap between the micrometer and nanometer ranges. The first is associated with 500 nm spatial resolution and is based on a pump–probe architecture using two laser sources, one for mid-infrared excitation (the pump) and the other one for measuring the photothermal effect (the probe) [158].

The lateral resolution of such a microscope is around 500 nm [159]. The second configuration combines an atomic force microscope and IR lasers [160,161] and produces a spatial resolution of 10 nm [162,163]. Several publications show that these two techniques can be applied to characterize abnormal deposits in tissues [164,165]. Using NanoIR spectroscopies, the complete set of data collected at the nanometer scale suggests that cystinosis is related to the pathogenesis of rectangular crystals of cysteine and not cystine [164].

Structural and chemical information is also available from synchrotron radiation [166–172] or electrons [102,103] as probes. The beam of a synchrotron radiation source can be focused down to the micrometer or even nanometer scale, allowing localised analyses [173,174]. Current research efforts are aimed not only at measuring the abnormal elemental distributions associated with various diseases, but also

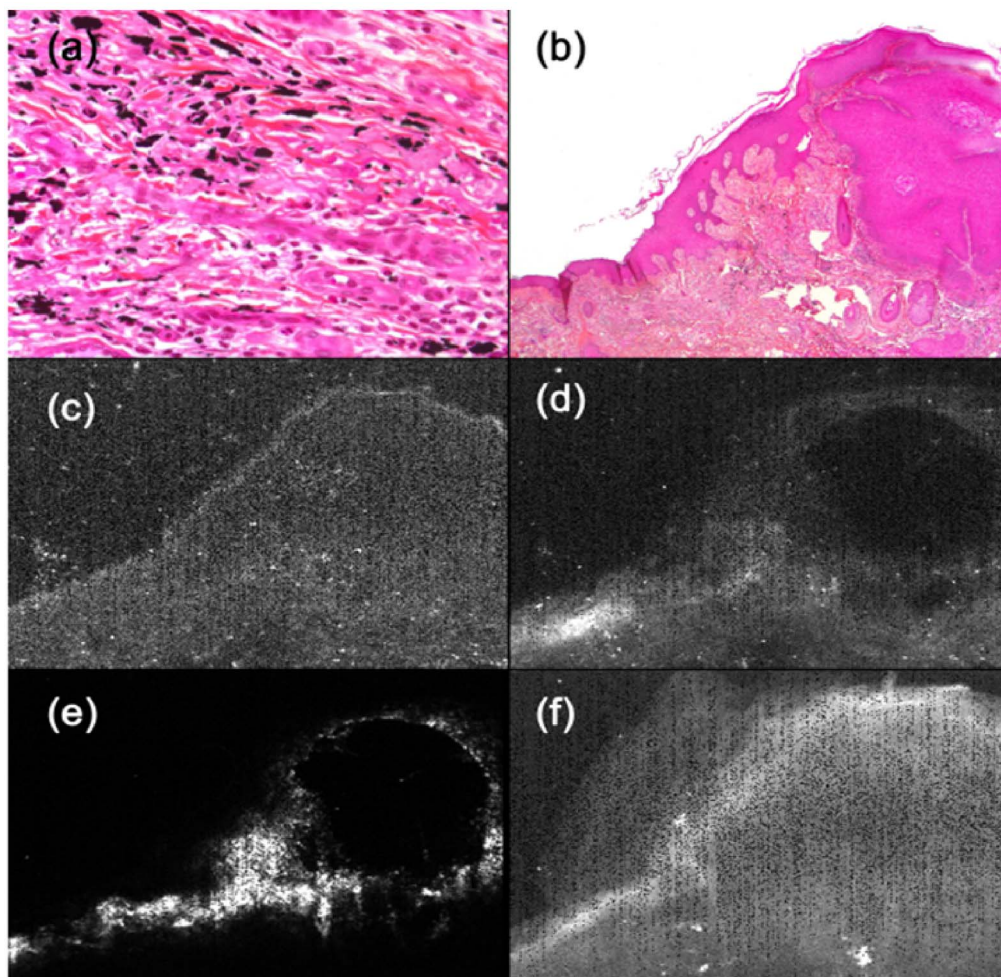


Figure 16. Optical microscopy and XRF correlation: Optical microscopy, showing mainly black ink in the superficial and deep dermis, with little, dispersed, and less visible, pink ink: (a) Hematoxylin-eosin-saffron (HES)-stained ($\times 400$) (b) HES-stained ($\times 25$). XRF analysis: The main elements observed are (c) Ca, (d) Fe (e) Ti and (f) Zn (from Colboc *et al.* [32]).

at suggesting or revealing possible biological mechanisms underlying the observations [175–179]. As a recent example, we have proposed a new, high-sensitivity technique based on synchrotron deep UV microspectroscopy with a submicrometre spatial resolution for the diagnosis of oxalate-mediated kidney diseases and an understanding of their physiopathology [172].

Finally, it is worth mentioning that it is possible to model nanometer scale material characteristics with theoretical approaches based on Density Functional Theory (DFT) calculations [180,181], which are

particularly effective in the case of nanomaterials [182–184]. It is now possible to predict nanocrystal morphology [185,186] or model the adsorption of small molecules at their surface [187–190]. Quantum chemical calculations can also be used to understand competition between the different complexation reactions and propose possible new and more efficient phosphate and oxalate sequestrants to prevent the formation of nanometer scale pathological calcifications [191].

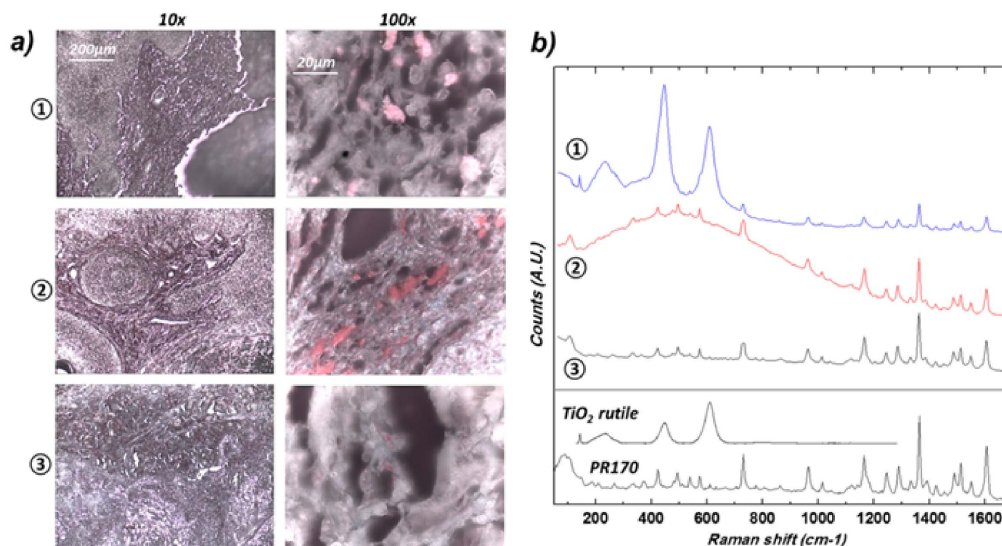


Figure 17. Optical micrographs of the three samples at two different magnifications (10× and 100×) revealing the presence of micron size red pigment clusters. Note the heterogeneous and lighter aspect of the red pigment, suggesting the presence of NPs of TiO₂. (b) Corresponding Raman spectra. Reference spectra are also given as comparison: PR170 dye sample (Kremer) and rutile (TiO₂) downloaded from the RRUFF database (from Colboc *et al.* [32]).

6. Conclusion

This contribution considers therapeutic nanomaterials dedicated to disease treatment, pathology-induced nanomaterials, and finally pathologies induced by deliberately injected nanomaterials related to tattooing. Clearly each nanomaterial family provides enough subject matter for a book!

Although the number of cited publications is limited, this concise review clearly demonstrates that the synthesis, and characterization, of nanomaterials, and understanding their interactions with biological tissues, constitute major challenges [192].

Conflicts of interest

The author has no conflict of interest to declare.

Acknowledgments

It is a great honour to have the opportunity to work and to develop special relationship with Dr. M. Daudon, Professor E. Letavernier, Dr. V. Frochot and Professor J. P. Haymann.

Also, It is a great honour to thank all the people who have played a significant role in the construction of this interface between physics, chemistry and medicine : Dr. X. Carpentier (Nice Hospital), Dr. Ch. Chappard (Lariboisière Hospital), Professor P. Conort (La Pitié-Salpêtrière Hospital), Dr. P. Dorfmueller (La Pitié-Salpêtrière Hospital), Dr. E. Estève (Tenon Hospital), Professor D. Hannouche (Lariboisière Hospital), Professor P. Jungers (Necker Hospital), Professor B. Knebelman (Necker Hospital), Dr. E. A. Korng (Lariboisière Hospital), Professor F. Liote (Lariboisière Hospital), Dr. M. Livrozet (Tenon Hospital), Professor M. Mathonnet (Limoges Hospital), Professor P. Méria (Saint-Louis Hospital), Dr. C. Nguyen (Lariboisière Hospital), Dr. J. Rode (Tenon Hospital), Professor P. Ronco (Tenon Hospital), Dr. I. Tostivint (La Pitié-Salpêtrière Hospital), Professor O. Traxer (Tenon Hospital) and Professor J. C. Williams (Department of Anatomy and Cell Biology, Indiana University School of Medicine, Indianapolis, Indiana, USA) for providing samples and useful discussions.

Also, regarding the physicochemistry, this research could not have been performed without the scientific advice of Dr. P.-A. Albouy (LPS), Dr. G. André (LLB), Dr. A. Bianchi (INSERM-U7561), Dr. P. Chevallier (LURE), Dr. A. Cousson (LLB), Dr. P. Dumas (SOLEIL Synchrotron), Professor M. Duer (Department of Chemistry, University of Cambridge, United kingdom), Dr. E. El Kaim (SOLEIL Synchrotron), Dr. B. Fayard (LPS-ESRF), Dr. E. Foy (Laboratoire Pierre-Süe), Dr. J.-L. Hazemann (ESRF), Dr. L. Hennet (CEMHTI), Dr. F. Jamme (SOLEIL Synchrotron), Dr. A. Lebail (Laboratoire des Fluorures), Dr. F. Lenaour (Hôpital Paul Brousse), Dr. O. Mathon (ESRF), Dr. K. Medjoubi (SOLEIL Synchrotron), Dr. G. Matzen (CEMHTI), Dr. C. Mocuta (SOLEIL Synchrotron), Dr. R. Papoular (CEA), Dr. P. Reboul, (UMR 7561), Dr. M. Réfrégiers (SOLEIL Synchrotron), Dr. S. Reguer (SOLEIL Synchrotron), Dr. D. Reid (Department of Chemistry, University of Cambridge), Dr. S. Rouzière (LPS), Dr. S. Kašćáková (Hôpital Paul Brousse), Dr. J.-P. Samama (SOLEIL Synchrotron), Dr. C. Sandt (SOLEIL Synchrotron), Dr. M. C. Schanne-Klain (LOB, Polytechnique), Dr. D. Reid (Department of chemistry, Cambridge University, United kingdom), Dr. A. Somogi (SOLEIL Synchrotron), Dr. D. Thiaudière (SOLEIL Synchrotron), Dr. E. Véron (CEMHTI) and Dr. R. Weil (LPS).

References

- [1] S. K. Murthy, *Int. J. Nanomedicine*, 2007, **2**, 129-141.
- [2] S. Chen, Q. Zhang, Y. Hou, J. Zhang, X.-J. Liang, *Eur. J. Nanomed.*, 2013, **5**, 61-79.
- [3] W. Lin, *Chem. Rev.*, 2015, **115**, 10407-10409.
- [4] S. Soares, J. Sousa, A. Pais, C. Vitorino, *Front. Chem.*, 2018, **6**, article no. 360.
- [5] J. Potocnik, *Official Journal of the European Union*, 2011, **2011**, article no. 2011/696/EU.
- [6] Z. Yuan, Y. Pan, R. Cheng, L. Sheng, W. Wu, G. Pan, Q. Feng, W. Cui, *Nanotechnology*, 2016, **27**, article no. 245101.
- [7] X. Yang, M. Yang, B. Pang, M. Vara, Y. Xia, *Chem. Rev.*, 2015, **115**, 10410-10488.
- [8] K.-M. Weltring, N. Gouze, N. Martin, I. Baanante, F. Gramatica, *Research and Innovation Agenda For Nanomedicine*, ETPN Association, France, 2016-2030 pages.
- [9] C. Sanchez, Ph. Belleville, M. Popall, L. Nicole, *Chem. Soc. Rev.*, 2011, **40**, 696-753.
- [10] L. Nicole, Ch. Laberty-Robert, L. Rozes, C. Sanchez, *Nanoscale*, 2014, **6**, 6267-6292.
- [11] E. Esteve, S. Reguer, C. Boissière, C. Chanéac, G. Lugo, Ch. Jouanneau, C. Mocuta, D. Thiaudière, N. Leclercq, B. Leyh, J.-F. Greisch, J. Berthault, M. Daudon, P. Ronco, D. Bazin, *J. Synchrotron Radiat.*, 2017, **24**, 991-999.
- [12] M. Hembury, C. Chiappini, S. Bertazzo, T. Kalber, G. L. Drisko, O. Ogunlade, S. Walker-Samuel, S. K. Krishna, C. Jumeaux, P. Beard, C. S. S. R. Kumar, A. E. Porter, M. F. Lythgoe, C. Boissière, C. Sanchez, M. M. Stevens, *Proc. Natl Acad. Sci. USA*, 2015, **112**, 1959-1964.
- [13] D. Bazin, M. Daudon, C. Combes, C. Rey, *Chem. Rev.*, 2012, **112**, 5092-5120.
- [14] D. Bazin, M. Daudon, *J. Phys. D: Appl. Phys.*, 2012, **45**, article no. 383001.
- [15] T. Oyama, T. Sano, T. Hikino, Q. Xue, K. Iijima, T. Nakajima, F. Koerner, *Virchows Arch.*, 2002, **440**, 267-273.
- [16] A. Ben Lakhdar, M. Daudon, M. C. Matthieu, A. Kellum, C. Balleyguier, D. Bazin, *C. R. Chim.*, 2016, **19**, 1610-1624.
- [17] E. J. Espinosa-Ortiz, B. H. Eisner, D. Lange, R. Gerlach, *Nat. Rev. Urol.*, 2019, **16**, 35-53.
- [18] M. Daudon, M. Petay, S. Vimont, A. Deniset, F. Tielens, J.-Ph. Haymann, E. Letavernier, V. Frochot, D. Bazin, *C. R. Chim.*, 2022, **25**, no. S1, Online first.
- [19] D. Bazin, R. J. Papoular, E. Elkaim, R. Weil, D. Thiaudière, C. Pisapia, B. Ménez, N. S. Hwang, F. Tielens, M. Livrozet, E. Boudierlique, J.-Ph. Haymann, E. Letavernier, L. Hennet, V. Frochot, M. Daudon, *C. R. Chim.*, 2022, **25**, no. S1, Online first.
- [20] M. Daudon, P. Jungers, D. Bazin, *N. Engl. J. Med.*, 2008, **359**, 100-102.
- [21] M. Daudon, P. Jungers, D. Bazin, *N. Engl. J. Med.*, 2009, **360**, 1680-1681.
- [22] M. Daudon, D. Bazin, G. André, P. Jungers, A. Cousson, P. Chevallier, E. Véron, G. Matzen, *J. Appl. Cryst.*, 2009, **42**, 109-115.
- [23] A. Dessombz, E. Letavernier, J.-Ph. Haymann, D. Bazin, M. Daudon, *J. Urol.*, 2015, **193**, 1564-1569.
- [24] E. Boudierlique, E. Tang, J. Perez, H.-K. Ea, F. Renaudin, A. Coudert, S. Vandermeersch, D. Bazin, J.-Ph. Haymann, C. Saint-Jacques, V. Frochot, M. Daudon, E. Letavernier, *C. R. Chim.*, 2022, **25**, no. S1, Online first.
- [25] F. Meiouet, S. El Kabbaj, M. Daudon, *C. R. Chim.*, 2022, **25**, no. S1, Online first.
- [26] D. Bazin, J.-P. Haymann, E. Letavernier, J. Rode, M. Daudon, *Presse Med.*, 2014, **43**, 135-148.
- [27] D. Bazin, E. Letavernier, J.-P. Haymann, P. Méria, M. Daudon, *Prog. Urol.*, 2016, **26**, 608-618.
- [28] D. Bazin, M. Daudon, V. Frochot, J.-Ph. Haymann, E. Letavernier, *C. R. Chim.*, 2022, **25**, no. S1, Online first.
- [29] G. Kyriakou, A. Kyriakou, Th. Fotas, *Actas Dermo-Sifiliogr.*, 2021, **112**, 907-909.
- [30] S. Gaudron, M.-C. Ferrier-Le Bouëdec, F. Franck, M. D'Incan, *Contact Derm.*, 2014, **72**, 97-105.
- [31] J. Serup, K. Hutton Carlsen, N. Dommershausen, M. Sepehri, B. Hesse, C. Seim, A. Luch, I. Schreiber, *Contact Derm.*, 2020, **82**, 73-82.
- [32] H. Colboc, D. Bazin, P. Moguelet, S. Reguer, R. Amode, C. Jouanneau, I. Lucas, L. Deschamps, V. Descamps, N. Kluger, *J. Eur. Acad. Dermatol. Venereol.*, 2020, **34**, e313-e315.
- [33] S. Pitz, R. Jahn, L. Frisch, A. Duis, N. Pfeiffer, *Br. J. Ophthalmol.*, 2002, **86**, 397-399.

- [34] T. J. Webster, *Int. J. Nanomed.*, 2006, **1**, 115-116.
- [35] Y. Min, J. M. Caster, M. J. Eblan, A. Z. Wang, *Chem. Rev.*, 2015, **115**, 11147-11190.
- [36] D. W. Deamer, *FASEB J.*, 2010, **24**, 1308-1310.
- [37] L. Zhang, F. X. Gu, J. M. Chan, A. Z. Wang, R. S. Langer, O. C. Farokhzad, *Clin. Pharmacol. Ther.*, 2008, **83**, 761-769.
- [38] S. M. Janib, A. S. Moses, J. A. MacKay, *Adv. Drug Deliv. Rev.*, 2010, **30**, 1052-1063.
- [39] E. R. Evans, P. Bugga, V. Asthana, R. Drezek, *Mater. Today*, 2018, **21**, 673-685.
- [40] M. Vallet-Regí, B. González, I. Izquierdo-Barba, *Int. J. Mol. Sci.*, 2019, **20**, article no. 3806.
- [41] R. Singh, M. S. Smitha, S. P. Singh, *J. Nanosci. Nanotechnol.*, 2014, **14**, 4745-4756.
- [42] U. Kadiyala, N. A. Kotov, J. S. Vanepps, *Curr. Pharm. Des.*, 2018, **24**, 896-903.
- [43] M. Yadid, R. Feiner, T. Dvir, *Nano Lett.*, 2019, **19**, 2198-2206.
- [44] O. V. Salata, *J. Nanobiotechnology*, 2004, **2**, article no. 3.
- [45] M. Jeyaraj, S. Gurunathan, M. Qasim, M.-H. Kang, J.-H. Kim, *Nanomaterials*, 2019, **9**, article no. 1719.
- [46] M. Faustini, D. Grosso, C. Boissière, R. Backov, C. Sanchez, *J. Sol-Gel Sci. Technol.*, 2014, **70**, 216-226.
- [47] C. Sanchez, L. Rozes, F. Ribot, C. Laberty-Robert, D. Grosso, C. Sassoey, C. Boissière, L. Nicole, *C. R. Chim.*, 2010, **13**, 3-39.
- [48] D. Grosso, F. Ribot, C. Boissière, C. Sanchez, *Chem. Soc. Rev.*, 2011, **40**, 829-848.
- [49] L. Zhu, M. Gharib, C. Becker, Y. Zeng, A. R. Ziefuß, L. Chen, A. M. Alkilany, Ch. Rehbock, S. Barcikowski, W. J. Parak, I. Chakraborty, *J. Chem. Educ.*, 2020, **97**, 239-243.
- [50] E. Esteve, "Applications des outils physicochimiques à la physiologie et physiopathologie rénale", PhD Thesis, Sorbonne university, Paris, France, 2021.
- [51] S. Rouzière, D. Bazin, M. Daudon, *C. R. Chim.*, 2016, **19**, 1404-1415.
- [52] D. Bazin, E. Foy, S. Reguer, S. Rouzière, B. Fayard, H. Colboc, J.-Ph. Haymann, M. Daudon, C. Mocuta, *C. R. Chim.*, 2022, **25**, no. S1, Online first.
- [53] D. Bazin, E. Letavernier, J.-P. Haymann, P. Méria, M. Daudon, *Prog. Urol.*, 2016, **26**, 608-618.
- [54] M. S. del Rio, A. Brunetti, B. Golosio, A. Somogyi, A. Simionovici, "XRAYLIB tables (X-ray fluorescence cross-section), Calculations using XRAYLIB 2.3 November 14", 2003, http://ftp.esrf.fr/pub/scisoft/xraylib/xraylib_tables_v2.3.pdf.
- [55] D. Bazin, X. Carpentier, I. Brocheriou, P. Dorfmüller, S. Aubert, Ch. Chappard, D. Thiaudière, S. Reguer, G. Waychunas, P. Jungers, M. Daudon, *Biochimie*, 2009, **91**, 1294-1300.
- [56] S. Reguer, C. Mocuta, D. Thiaudière, M. Daudon, D. Bazin, *C. R. Chim.*, 2016, **19**, 1424-1431.
- [57] A. S. Prasad, J. A. Halsted, M. Nadimi, *Am. J. Med.*, 1961, **31**, 532-546.
- [58] J. Olechnowicz, A. Tinkov, A. Skalny, J. Suliburska, *J. Physiol. Sci.*, 2018, **68**, 19-31.
- [59] E. E. M. Manders, F. J. Verbeek, J. A. Aten, *J. Microsc.*, 2003, **169**, 375-382.
- [60] Q. Li, A. Lau, T. J. Morris, L. Guo, C. B. Fordyce, E. F. Stanley, *J. Neurosci.*, 2004, **24**, 4070-4081.
- [61] E. Esteve, D. Bazin, C. Jouanneau, S. Rouzière, A. Bataille, A. Kellum, K. Provost, C. Mocuta, S. Reguer, P. Ronco, J. Rehr, J.-P. Haymann, E. Letavernier, A. Hertig, *C. R. Chim.*, 2016, **19**, 1580-1585.
- [62] E. Esteve, D. Bazin, C. Jouanneau, S. Rouzière, A. Bataille, A. Kellum, K. Provost, C. Mocuta, S. Reguer, P. Ronco, J. Rehr, J.-P. Haymann, E. Letavernier, A. Hertig, *C. R. Chim.*, 2016, **19**, 1586-1589.
- [63] D. Bazin, M. Daudon, P. Chevallier, S. Rouzière, E. Elkaim, D. Thiaudière, B. Fayard, E. Foy, P. A. Albouy, G. André, G. Matzen, E. Véron, *Ann. Biol. Clin.*, 2006, **64**, 125-139.
- [64] D. Bazin, M. Daudon, *Ann. Biol. Clin.*, 2015, **73**, 517-534.
- [65] M. Daudon, D. Bazin, *J. Phys. Conf. Ser.*, 2013, **425**, article no. 022006.
- [66] D. Bazin, M. Daudon, *J. Spectral Imaging*, 2019, **8**, article no. a16.
- [67] D. Bazin, E. Letavernier, J. P. Haymann, V. Frochot, M. Daudon, *Ann. Biol. Clin.*, 2020, **78**, 349-362.
- [68] D. Bazin, V. Frochot, J.-Ph. Haymann, E. Letavernier, M. Daudon, *C. R. Chim.*, 2022, **25**, no. S1, Online first.
- [69] M. Daudon, C. A. Bader, P. Jungers, *Scanning Microsc.*, 1993, **7**, 1081-1104.
- [70] M. Daudon, P. Jungers, D. Bazin, *AIP Conf. Proc.*, 2008, **1049**, 199-215.
- [71] M. Daudon, H. Bouzidi, D. Bazin, *Urol. Res.*, 2010, **38**, 459-467.
- [72] M. Daudon, A. Dessombz, V. Frochot, E. Letavernier, J.-Ph. Haymann, P. Jungers, D. Bazin, *C. R. Chim.*, 2016, **19**, 1470-1491.
- [73] A. Dessombz, P. Méria, D. Bazin, M. Daudon, *PLoS One*, 2012, **7**, article no. e51691.
- [74] A. Dessombz, P. Méria, D. Bazin, E. Foy, S. Rouzière, R. Weil, M. Daudon, *Prog. Urol.*, 2011, **21**, 940-945.
- [75] M. Mathonnet, A. Dessombz, D. Bazin, R. Weil, F. Triponez, M. Pusztaszeri, M. Daudon, *C. R. Chim.*, 2016, **19**, 1672-1678.
- [76] J. Guerlain, S. Perie, M. Lefevre, J. Perez, S. Vandermeersch, Ch. Jouanneau, L. Huguet, V. Frochot, E. Letavernier, R. Weil, S. Rouzière, D. Bazin, M. Daudon, J. P. Haymann, *PLoS One*, 2019, **14**, article no. e0224138.
- [77] L. Henry, D. Bazin, C. Policar, J.-Ph. Haymann, M. Daudon, V. Frochot, M. Mathonnet, *C. R. Chim.*, 2022, **25**, no. S1, Forthcoming.
- [78] H. Colboc, Ph. Moguelet, E. Letavernier, V. Frochot, J.-F. Bernaudin, R. Weil, S. Rouzière, P. Seneth, C. Bachmeyer, N. Laporte, I. Lucas, V. Descamps, R. Amodek, F. Brunet-Possentik, N. Kluger, L. Deschamps, A. Dubois, S. Reguer, A. Somogyi, K. Medjoubi, M. Refregiers, M. Daudon, D. Bazin, *C. R. Chim.*, 2022, **25**, no. S1, Online first.
- [79] M. Petay, M. Cherfan, A. Deniset, E. Boudierlique, S. Reguer, A. Dazzi, J. Mathurin, M. Daudon, V. Frochot, J.-Ph. Haymann, E. Letavernier, D. Bazin, *C. R. Chim.*, 2022, **25**, no. S1, Forthcoming.
- [80] C. Nguyen, H.-K. Ea, D. Bazin, M. Daudon, F. Lioté, *Arthritis Rheum.*, 2010, **62**, 2829-2830.
- [81] H.-K. Ea, C. Nguyen, D. Bazin, A. Bianchi, J. Guicheux, P. Reboul, M. Daudon, F. Lioté, *Arthritis Rheum.*, 2010, **63**, 10-18.
- [82] C. Nguyen, H. K. Ea, D. Thiaudière, S. Reguer, D. Hannouche, M. Daudon, F. Lioté, D. Bazin, *J. Syn. Rad.*, 2011, **18**, 475-480.
- [83] H.-K. Ea, V. Chobaz, C. Nguyen, S. Nasir, P. van Lent, M. Daudon, A. Dessombz, D. Bazin, G. McCarthy, B. Jolles-

- Haerberli, A. Ives, D. Van Linthoudt, A. So, F. Lioté, N. Busso, *PLoS One*, 2013, **8**, article no. e57352.
- [84] A. Dessombz, C. Nguyen, H.-K. Ea, S. Rouzière, E. Foy, D. Hannouche, S. Réguer, F.-E. Picca, D. Thiaudière, F. Lioté, M. Daudon, D. Bazin, *J. Trace Elem. Med. Biol.*, 2013, **27**, 326-333.
- [85] Ch. Nguyen, D. Bazin, M. Daudon, A. Chatron-Colliet, D. Hannouche, A. Bianchi, D. Côme, A. So, N. Busso, F. Lioté, H.-K. Ea, *Arthritis Res. Ther.*, 2013, **15**, article no. R103.
- [86] H.-K. Ea, A. Gauffenic, Q. D. Nguyen, N. G. Pham, O. Olivier, V. Frochot, D. Bazin, N. H. Le, C. Marty, A. Ostertag, M. Cohen-Solal, J.-D. Laredo, P. Richette, Th. Bardin, *Arthritis Rheumatol.*, 2021, **73**, 324-329.
- [87] A. Gauffenic, D. Bazin, Ch. Combes, M. Daudon, H.-K. Ea, C. R. Chim., 2022, **25**, no. S1, Online first.
- [88] X. Carpentier, D. Bazin, Ch. Combes, A. Mazouyes, S. Rouzière, P.A. Albouy, E. Foy, M. Daudon, *J. Trace Elem. Med. Biol.*, 2011, **25**, 160-165.
- [89] A. Randall, *N. Engl. J. Med.*, 1936, **214**, 234-242.
- [90] M. Daudon, *Ann. Urol. (Paris)*, 2005, **39**, 209-231.
- [91] K. Bouchireb, O. Boyer, C. Pietrement, H. Nivet, H. Martelli, O. Dunand, F. Nobili, G. L. Sylvie, P. Niaudet, R. Salomon, M. Daudon, *Nephrol. Dial. Transplant.*, 2012, **27**, 1529-1534.
- [92] Ch. Rey, Ch. Combes, Ch. Drouet, H. Sfihi, A. Barroug, *Mater. Sci. Eng. C*, 2007, **27**, 198-205.
- [93] C. Rey, B. Collins, T. Goehl, I. R. Dickson, M. J. Glimcher, *Calcif. Tissue Int.*, 1989, **45**, 157-164.
- [94] Ch. Combes, Ch. Rey, *Minerals*, 2016, **6**, article no. 34.
- [95] M. Daudon, O. Traxer, P. Jungers, D. Bazin, *AIP Conf. Proc.*, 2007, **900**, 26-34.
- [96] X. Carpentier, D. Bazin, P. Jungers, S. Reguer, D. Thiaudière, M. Daudon, *J. Synchrotron Radiat.*, 2010, **17**, 374-379.
- [97] M. Daudon, O. Traxer, J. C. Williams, D. Bazin, "Randall's plaque", in *Urinary Tract Stone Disease* (N. P. Rao, G. M. Preminger, J. P. Kavangh, eds.), Springer, ISBN 978-1-84800-361-3.
- [98] E. Letavernier, D. Bazin, M. Daudon, *C. R. Chim.*, 2016, **19**, 1456-1460.
- [99] D. Bazin, E. Letavernier, Ch. Jouanneau, P. Ronco, Ch. Sandt, P. Dumas, G. Matzen, E. Véron, J.-Ph. Haymann, O. Traxer, P. Conort, M. Daudon, *C. R. Chim.*, 2016, **19**, 1461-1469.
- [100] E. Letavernier, G. Kauffenstein, L. Huguet, N. Navasiolava, E. Boudierlique, E. Tang, L. Delaitre, D. Bazin, M. de Frutos, C. Gay, J. Perez, M. C. Verpont, J.-Ph. Haymann, V. Pomozi, J. Zoll, O. Le Saux, M. Daudon, G. Leftheriotis, L. Martin, *J. Am. Soc. Nephrol.*, 2018, **29**, 2337-2347.
- [101] H. Bilbault, J. Perez, L. Huguet, S. Vandermeersch, S. Placier, N. Tabibzadeh, V. Frochot, E. Letavernier, D. Bazin, M. Daudon, J.-P. Haymann, *Sci. Rep.*, 2018, **8**, article no. 16319.
- [102] C. Verrier, D. Bazin, L. Huguet, O. Stéphan, A. Gloter, M.-Ch. Verpont, V. Frochot, J.-Ph. Haymann, I. Brocheriou, O. Traxer, M. Daudon, E. Letavernier, *J. Urol.*, 2016, **196**, 1566-1574.
- [103] C. Gay, E. Letavernier, M.-Ch. Verpont, M. Walls, D. Bazin, M. Daudon, N. Nassif, O. Stephan, M. de Frutos, *ACS Nano*, 2020, **14**, 1823-1836.
- [104] S. R. Khan, *C. R. Chim.*, 2022, **25**, no. S1, Online first.
- [105] E. Van de Perre, D. Bazin, V. Estrade, E. Boudierlique, K. M. Wissing, M. Daudon, E. Letavernier, *C. R. Chim.*, 2022, **25**, no. S1, Online first.
- [106] D. Bazin, C. Chappard, C. Combes, X. Carpentier, S. Rouzière, G. André, G. Matzen, M. Allix, D. Thiaudière, S. Reguer, P. Jungers, M. Daudon, *Osteoporosis Int.*, 2009, **20**, 1065-1075.
- [107] M. U. Nysten, E. D. Eanes, K. A. Omnell, *J. Cell Biol.*, 1963, **18**, 109-123.
- [108] P. D. Frazier, *J. Ultrastruct. Res.*, 1968, **22**, 1-11.
- [109] H. Colboc, Th. Bettuzzi, M. Badrignans, D. Bazin, A. Boury, E. Letavernier, V. Frochot, E. Tang, Ph. Moguelet, N. Ortonne, N. de Prost, S. Ingen-Housz-Oro, M. Daudon, *C. R. Chim.*, 2022, **25**, no. S1, Online first.
- [110] M. Daudon, O. Traxer, P. Conort, B. Lacour, P. Jungers, *J. Am. Soc. Nephrol.*, 2006, **17**, 2026-2033.
- [111] M. Daudon, P. Jungers, *Feuill. Biol.*, 2001, **42**, 37-39.
- [112] M. Daudon, B. Lacour, P. Jungers, *Urol. Res.*, 2006, **34**, 193-199.
- [113] F. Damay, D. Bazin, M. Daudon, G. André, *C. R. Chim.*, 2016, **19**, 1432-1438.
- [114] M. Daudon, E. Letavernier, R. Weil, E. Véron, G. Matzen, G. André, D. Bazin, *C. R. Chim.*, 2016, **19**, 1527-1534.
- [115] K. Sakhaee, B. Adams-Huet, O. W. Moe, C. Y. Pak, *Kidney Int.*, 2002, **62**, 971-979.
- [116] D. Bazin, M. Daudon, G. André, R. Weil, E. Véron, G. Matzen, *J. Appl. Cryst.*, 2014, **47**, 719-725.
- [117] E. Letavernier, O. Traxer, J.-P. Haymann, D. Bazin, M. Daudon, *Prog. Urol.*, 2012, **22**, F119-F123.
- [118] J. P. Haymann, M. Livrozet, J. Rode, S. Doizi, O. Traxer, V. Frochot, E. Letavernier, D. Bazin, M. Daudon, *Prog. Urol. - FMC*, 2021, **31**, F1-F7.
- [119] M. Livrozet, S. Vandermeersch, L. Mesnard, E. Thioulouse, J. Jaubert, J.-J. Boffa, J.-P. Haymann, L. Baud, D. Bazin, M. Daudon, E. Letavernier, *PLoS One*, 2014, **9**, article no. e102700.
- [120] D. S. Milliner, *Endocrinol. Metab. Clin. North Am.*, 1990, **19**, 889-907.
- [121] E. A. Bresnitz, B. L. Strom, *Epidemiol. Rev.*, 1983, **5**, 124-156.
- [122] G. W. Hunninghake, U. Costabel, M. Ando, R. Baughman, J. F. Cordier, R. Du Bois, A. Eklund, M. Kitachi, J. Lynch, G. Rizzato, C. Rose, O. Selroos, G. Semenzato, O. P. Sharma, *Am. J. Respir. Crit. Care Med.*, 1999, **160**, 736-755.
- [123] N. H. Bell, P. H. Stern, E. Pantzer, T. K. Sinha, H. F. Deluca, *J. Clin. Investig.*, 1979, **64**, 218-225.
- [124] N. Saidenberg-Kermanac'h, L. Semerano, H. Nunes, D. Sadoun, X. Guillot, M. Boubaya, N. Naggara, D. Valeyre, M.-Ch. Boissier, *Arthritis Res. Ther.*, 2014, **16**, article no. R78.
- [125] E. V. Arkema, Y. C. Cozier, *Ther. Adv. Chronic Dis.*, 2018, **9**, 227-240.
- [126] E. V. Arkema, J. Grunewald, S. Kullberg, A. Eklund, J. Askling, *Eur. Respir. J.*, 2016, **48**, 1690-1699.
- [127] H. Colboc, D. Bazin, Ph. Moguelet, V. Frochot, R. Weil, E. Letavernier, Ch. Jouanneau, C. Frances, C. Bachmeyer, J.-F. Bernaudin, M. Daudon, *C. R. Chim.*, 2016, **19**, 1631-1641.
- [128] I. Schreiber, B. Hesse, Ch. Seim, H. Castillo-Michel, J. Villanova, P. Laux, N. Dreiaek, R. Penning, R. Tucoulou, M. Cotte, A. Luch, *Sci. Rep.*, 2017, **7**, article no. 11395.
- [129] I. Schreiber, B. Hesse, Ch. Seim, H. Castillo-Michel, L. Anklam, J. Villanova, N. Dreiaek, A. Lagrange, R. Penning,

- Ch. De Cuyper, R. Tucoulou, W. Bäuml, M. Cotte, A. Luch, *Part. Fibre Toxicol.*, 2019, **16**, article no. 33.
- [130] N. Kluger, *Curr. Probl. Dermatol.*, 2015, **48**, 6-20.
- [131] G. Forte, F. Petrucci, A. Cristaudo, B. Bocca, *Sci. Total Environ.*, 2009, **407**, 5997-6002.
- [132] P. Minghetti, U. M. Musazzi, R. Dorati, P. Rocco, *Sci. Total Environ.*, 2019, **651**, 634-637.
- [133] B. Battistini, F. Petrucci, I. De Angelis, C. M. Failla, B. Bocca, *Chemosphere*, 2020, **245**, article no. 125667.
- [134] M. Arl, D. J. Nogueira, J. Schweitzer Köerich, N. M. Justino, D. S. Vicentini, W. G. Matias, *J. Hazard. Mater.*, 2019, **364**, 548-561.
- [135] T. Høgsberg, K. Loeschner, D. Löf, J. Serup, *Br. J. Dermatol.*, 2011, **165**, 1210-1218.
- [136] J. Tang, L. Xiong, S. Wang, J. Wang, L. Liu, J. Li, F. Yuan, T. Xi, *J. Nanosci. Nanotechnol.*, 2009, **9**, 4924-4932.
- [137] M. Daudon, D. Bazin, *C. R. Chim.*, 2016, **19**, 1416-1423.
- [138] A. Dessombz, D. Bazin, P. Dumas, C. Sandt, J. Sule-Suso, M. Daudon, *PLoS One*, 2012, **6**, article no. e28007.
- [139] I. T. Lucas, D. Bazin, M. Daudon, *C. R. Chim.*, 2022, **25**, no. S1, Online first.
- [140] S. Tamosaityte, M. Pucetaite, A. Zelvy, S. Varvuolyte, V. Hendrixson, V. Sablinskas, *C. R. Chim.*, 2022, **25**, no. S1, Online first.
- [141] B. J. Yakes, T. J. Michael, M. Perez-Gonzalez, B. P. Harp, *J. Raman Spectrosc.*, 2017, **48**, 736-743.
- [142] O. Olsen, in *Current Problems in Dermatology* (J. Serup, N. Kluger, W. Baumler, eds.), vol. 48, Karger, Basel, 2015, 158.
- [143] V. De Matteis, M. F. Cascione, V. Brunetti, Ch. C. Toma, R. Rinaldi, *Toxicol. In Vitro*, 2016, **37**, 201-210.
- [144] J. Moonen, J. Slot, L. Lefferts, D. Bazin, H. Dexpert, *Physica B*, 1995, **208 & 209**, 689-690.
- [145] D. Bazin, D. Sayers, J. Rehr, *J. Phys. Chem. B*, 1997, **101**, 11040-11050.
- [146] D. Bazin, D. Sayers, J. J. Rehr, C. Mottet, *J. Phys. Chem. B*, 1997, **101**, 5332-5336.
- [147] D. Bazin, J. J. Rehr, *J. Phys. Chem. B*, 2003, **107**, 12398-12402.
- [148] D. Bazin, S. Reguer, D. Vantelon, J.-Ph. Haymann, E. Letavernier, V. Frochot, M. Daudon, E. Esteve, H. Colboc, *C. R. Chim.*, 2022, **25**, no. S1, Online first.
- [149] U. Hauri, C. Hohl, *Tattooed Skin and Health*, Karger Publishers, 2015, 164-169 pages.
- [150] V. Frochot, D. Bazin, E. Letavernier, Ch. Jouanneau, J.-Ph. Haymann, M. Daudon, *C. R. Chim.*, 2016, **19**, 1565-1572.
- [151] Y. Luque, K. Louis, C. Jouanneau, S. Placier, E. Esteve, D. Bazin, E. Rondeau, E. Letavernier, A. Wolfroth, C. Gosset, A. Boueill, M. Burbach, P. Frère, M.-C. Verpont, S. Vandermeersch, D. Langui, M. Daudon, V. Frochot, L. Mesnard, *J. Am. Soc. Nephrol.*, 2017, **28**, 1723-1728.
- [152] M. Daudon, V. Frochot, D. Bazin, P. Jungers, *Drugs*, 2018, **78**, 163-201.
- [153] A.-L. Faucon, M. Daudon, V. Frochot, D. Bazin, B. Terris, V. Caudwell, *Kidney Int.*, 2018, **93**, 1251-1252.
- [154] E. Esteve, Y. Luque, J. Waeytens, D. Bazin, L. Mesnard, Ch. Jouanneau, P. Ronco, A. Dazzi, M. Daudon, A. Deniset-Besseau, *Anal. Chem.*, 2020, **92**, 7388-7392.
- [155] J. Zaworski, E. Boudierlique, D. Anglicheau, J.-P. Duong Van Huyen, V. Gnemmi, J.-B. Gibier, Y. Neugebauer, J.-Ph. Haymann, D. Bazin, V. Frochot, M. Daudon, E. Letavernier, *Kidney Int. Rep.*, 2020, **5**, 737-741.
- [156] G. Chebion, E. Bugni, V. Gerin, M. Daudon, V. Castiglione, *C. R. Chim.*, 2022, **25**, no. S1, Online first.
- [157] D. Bazin, I. T. Lucas, S. Rouzière, E. Elkaim, C. Mocuta, S. Réguer, D. G. Reid, J. Mathurin, A. Dazzi, A. Deniset, M. Petay, V. Frochot, J.-Ph. Haymann, E. Letavernier, M.-Ch. Verpont, E. Foy, E. Boudierlique, H. Colboc, M. Daudon, *C. R. Chim.*, 2022, **25**, no. S1, Forthcoming.
- [158] D. Fournier, F. Lepoutre, A. Boccara, *J. Phys.*, 1983, **44**, 479-482.
- [159] M. Kansiz, C. Prater, E. Dillon, M. Lo, J. Anderson, C. Marcott, A. Demissie, Y. Chen, G. Kunkel, *Microsc. Today*, 2020, **28**, 26-36.
- [160] A. Dazzi, F. Glotin, R. Carminati, *J. Appl. Phys.*, 2010, **107**, article no. 124519.
- [161] A. Dazzi, C. B. Prater, *Chem. Rev.*, 2017, **117**, 5146-5173.
- [162] J. Mathurin, A. Deniset-Besseau, D. Bazin, E. Dartois, M. Wagner, A. Dazzi, *J. Appl. Phys.*, 2022, **131**, article no. 010901.
- [163] J. Mathurin, "Nanospectroscopie infrarouge avancée : développements instrumentaux et applications", PhD Thesis, Université Paris Saclay, Paris, France, 2019.
- [164] D. Bazin, M. Rabant, J. Mathurin, M. Petay, A. Deniset-Besseau, A. Dazzi, Y. Su, E. P. Hesson, F. Tielens, F. Borondics, M. Livrozet, E. Boudierlique, J.-Ph. Haymann, E. Letavernier, V. Frochot, M. Daudon, *C. R. Chim.*, 2022, **25**, no. S1, Online first.
- [165] D. Bazin, E. Boudierlique, E. Tang, M. Daudon, J.-Ph. Haymann, V. Frochot, E. Letavernier, J. C. Williams Jr., J. E. Linge-mang, F. Borondics, *C. R. Chim.*, 2022, **25**, no. S1, Forthcoming.
- [166] S. Bohic, M. Cotte, M. Salomé, B. Fayard, M. Kuehbach, P. Cloetens, G. Martinez-Criado, R. Tucoulou, J. Susini, *Struct. Biol.*, 2012, **177**, 248-258.
- [167] S. Kaščáková, C. M. Kewish, S. Rouzière, F. Schmitt, R. Sobesky, J. Poupon, C. Sandt, B. Francou, A. Somogyi, D. Samuel, E. Jacquemin, A. Dubart-Kupperschmitt, T. H. Nguyen, D. Bazin, J.-C. DuclosVallée, C. Guettier, F. Le Naour, *J. Pathol. Clin. Res.*, 2016, **2**, 175-186.
- [168] F. Brunet-Possenti, L. Deschamps, H. Colboc, A. Somogyi, K. Medjoubi, D. Bazin, V. Descamps, *J. Eur. Acad. Dermatol. Venereol.*, 2018, **32**, e442-e443.
- [169] A. A. Guda, S. A. Guda, K. A. Lomachenko, M. A. Soldatov, I. A. Pankin, A. V. Soldatov, L. Braglia, A. L. Bugaev, A. Martini, M. Signorile, E. Groppo, A. Piovano, E. Borfecchia, C. Lamberti, *Cat. Today*, 2019, **336**, 3-21.
- [170] J. Timoshenko, B. R. Cuenya, *Chem. Rev.*, 2021, **121**, 882-961.
- [171] W.-H. Huang, W.-N. Sua, C.-L. Chen, C.-J. Lin, S.-C. Haw, J.-F. Lee, B. J. Hwang, *Appl. Surf. Sci.*, 2021, **562**, article no. 150127.
- [172] E. Estève, D. Buob, F. Jamme, Ch. Jouanneau, S. Kascakova, J. Ph. Haymann, E. Letavernier, L. Galmiche, P. Ronco, M. Daudon, D. Bazin, M. Réfrégiers, *J. Synchrotron Radiat.*, 2022, **29**, 214-223.
- [173] A. Sakdinawat, D. Attwood, *Nat. Photonics*, 2010, **4**, 840-848.
- [174] H. Rarback, D. Shu, S. C. Feng, H. Ade, J. Kirz, I. McNulty, *Rev. Sci. Instrum.*, 1988, **59**, 52-59.

- [175] M. L. Carvalho, C. Casaca, J. P. Marques, T. Pinheiro, A. S. Cunha, *X-ray Spectrom.*, 2001, **30**, 190-193.
- [176] L. J. Bauer, H. A. Mustafa, P. Zaslansky, I. Mantouvalou, *Acta Biomater.*, 2020, **109**, 142-152.
- [177] M. R. Gherase, D. E. B. Fleming, *Crystals*, 2020, **10**, article no. 12.
- [178] J. E. Penner-Hahn, "Technologies for detecting metals in single cells", in *Metallomics and the Cell* (L. Banci, ed.), Metal Ions in Life Sciences, vol. 12, Springer, Dordrecht, 2013.
- [179] R. Ortega, P. Cloetens, G. Devès, A. Carmona, S. Bohic, *PLoS ONE*, 2007, **2**, article no. e925.
- [180] P. Hohenberg, W. Kohn, *Phys. Rev. B*, 1964, **136**, 864-871.
- [181] R. O. Jones, *Rev. Mod. Phys.*, 2015, **87**, 897-923.
- [182] D. Bazin, F. Tielens, *Appl. Catal.*, 2015, **504**, 631-641.
- [183] F. Tielens, D. Bazin, *C. R. Chim.*, 2018, **21**, 174-181.
- [184] F. Tielens, J. Vekeman, D. Bazin, M. Daudon, *C. R. Chim.*, 2022, **25**, no. S1, Online first.
- [185] T. Debroise, T. Sedzik, J. Vekeman, Y. Su, C. Bonhomme, F. Tielens, *Cryst. Growth Des.*, 2020, **20**, 3807-3815.
- [186] T. Debroise, E. Colombo, G. Belletti, J. Vekeman, Y. Su, R. Pa-poular, N. S. Hwang, D. Bazin, M. Daudon, P. Quaino, F. Tielens, *Cryst. Growth Des.*, 2020, **20**, 2553-2561.
- [187] I. C. Oguz, H. Guesmi, D. Bazin, F. Tielens, *J. Phys. Chem. C*, 2019, **123**, 20314-20318.
- [188] N. Takagi, K. Ishimura, R. Fukuda, M. Ehara, S. Sakaki, *J. Phys. Chem. A*, 2019, **123**, 7021-7033.
- [189] N. Takagi, M. Ehara, S. Sakaki, *ACS Omega*, 2021, **6**, 4888-4898.
- [190] D. Bazin, J. Vekeman, Q. Wang, X. Deraet, F. De Proft, H. Guesmi, F. Tielens, *C. R. Chim.*, 2022, **25**, no. S3, Online first.
- [191] J. Vekeman, J. Torres, C. E. David, E. Van de Perre, K. M. Wissing, E. Letavernier, D. Bazin, M. Daudon, A. Pozdzik, F. Tielens, *Nanomaterials (Basel)*, 2021, **11**, article no. 1763.
- [192] C. Meunier, "Innovations thérapeutiques : évolutions et tendances", 2014, <https://www.college-de-france.fr/site/bernard-meunier/inaugural-lecture-2014-11-06-18h00.htm>.